Results of all the available archaeological and archaeometrical information on the excavation of Kara Tepe.

Evanthia Tsantini, Verònica Martínez and Josep M Gurt

Archaeometrical estudy of ceramic material from kiln 2

Introduction

In Uzbekistan a number of archaeometrical studies were done during the 1980's and early 90's using chemical and mineralogical analysis, notably by S. V. Vivdenko and A. Abdurazakov. The first analysed shards from a number of sites mostly dated to the Iron Age but also from the Kushan period at Jalangtush Tepe [Vivdenko 1987, 1987a, 1990, 1992, 1993, 1994 and 1996]. Abdurazakov also analysed a few sherds, mainly dated to the Bronze Age but including some from the Kushan period at sites such as Mirzakul' Tepe and Talashkan Tepe [Abdurazakov, Bezborodov et alii. 1963, Abdurazakov 1988, Abdurazakov 1996, Abdurazakov, Dzhalalova 1986, Abdurazakov 1987]. None of this work had the necessary continuation neither was based on the definition of Reference Groups (RG) of Paste Compositional Reference Units (PCRU) which is a fundamental process in the mark of provenience studies in order to attempt to locate the *origin* or the *production site* where the pottery was made [Picon, 1984; Buxeda *et al.*,1995].

The present work is centred to the study of production and possible local distribution of ceramics dated in the Kushan period sampled at one of the ceramic kilns of Kara Tepe (Table 1) (Figures 1, 2, 3, 4, 5, 6, 7, 8). It aims, also, to study the technological aspects of fabrication of these ceramics. In order to cover these subjects an archaeometric study of a total of 50 samples (Table 1) has been carried out by applying chemical and mineralogical techniques. The chemical composition has been determined by X-Ray Fluorescence (XRF), and the mineralogy has been investigated using X-Ray Diffraction (XRD). The analysed material can be divided into two basic categories: painted wares covered with a red, brown or almost black slip (CER) and common wares (CC) all of them dated to the Kushan or Kushano-Sassanid periods [E. Ariño, *et al*, 2006].

The analytical programme and methodology

XRF was performed using a Phillips PW 2400 spectrometer with a Rh excitation source. A portion of specimens were dried at 100°C for 24 h. Major and minor elements were determined by preparing duplicate of glassy pills using 0.3 g of powdered specimen in an alkaline fusion with lithium tetraborate at 1/20 dilution. Trace elements and Na_2O were determined by powdered pills made from 5 g of specimen mixed with Elvacite agglutinating placed over boric acid in an aluminium capsule and pressed for 60 s at 200 kN. The quantification of the concentrations was obtained by using a calibration line performed with 60 International Geological Standards (Hein *et al.*, 2002). The elements identified comprised Fe_2O_3 (as total Fe), Al_2O_3, MnO, P_2O_5, TiO_2, MgO, CaO, Na_2O, K_2O, SiO_2, Ba, Rb, Mo, Th, Nb, Pb, Zr, Y, Sr, Sn, Ce, Co, Ga, V, Zn, W, Cu, Ni and Cr. The loss on ignition (LOI) was determined by firing 0.3 g of dried specimen at 950°C for 3 h.

XRD analyses were carried out by using the same specimens prepared for XRF analysis. Measurements were performed using a Siemens D-500 diffractometer working with the Cu Kα radiation (λ=1.5406 Å), and graphite monochromator in the diffracted beam, at 1.2 kW (40 kV, 30 mA). Spectra were taken from 4 to 70°2Θ, at 1°2Θ/min (step size=0.05°2Θ; time=3 s). The evaluation of crystalline phases was carried out using the DIFFRACT/AT program by Siemens, which includes the Joint Committee of Powder Diffraction Standards (JCPDS) data bank.

CODE OF ANALYSIS	CODE OF INVENTORY	TYPE
TRZ001	TZ06KTH2UE11 4	PAINTED (red)
TRZ002	TZ06KTH2UE12 9	PAINTED
TRZ003	TZ06KTH2UE12 7	PAINTED (red)
TRZ004	TZ06KTH2UE11 2	COMMON WARE
TRZ005	TZ06KTH2UE9 2	PAINTED (red)
TRZ006	TZ06KTH2UE12 4	COMMON WARE
TRZ007	TZ06KTH2UE1 2	COMMON WARE
TRZ008	TZ06KTH2UE9 16	PAINTED (red)
TRZ009	TZ06KTH2UE9 1	COMMON WARE
TRZ010	TZ06KTH2UE9 9	COMMON WARE
TRZ011	TZ06KTH2UE1 7	COMMON WARE
TRZ012	TZ06KTH2UE1 3	PAINTED (red)
TRZ013	TZ06KTH2UE1 5	PAINTED (red)
TRZ014	TZ06KTH2UE11 3	PAINTED (red)
TRZ015	TZ06KTH2UE9 17	PAINTED (red)
TRZ016	TZ06KTH2UE12 8	COMMON WARE
TRZ017	TZ06KTH2UE9 8	COMMON WARE
TRZ018	TZ06KTH2UE12 10	PAINTED (red)
TRZ019	TZ06KTH2UE9 10	COMMON WARE
TRZ020	TZ06KTH2UE12 5	COMMON WARE
TRZ021	TZ06KTH2UE9 15	COMMON WARE
TRZ022	TZ06KTH2UE11 5	PAINTED (red)
TRZ023	TZ06KTH2UE9 19	COMMON WARE
TRZ024	TZ06KTH2UE9 3	PAINTED (red)
TRZ025	TZ06KTH2UE11 1	COMMON WARE
TRZ026	TZ06KTH2UE9 18	PAINTED (red)
TRZ027	TZ06KTH2UE9 4	PAINTED (red)
TRZ028	TZ06KTH2UE9 7	COMMON WARE
TRZ029	TZ06KTH2UE9 5	PAINTED (red)
TRZ030	TZ06KTH2UE12 3	COMMON WARE
TRZ031	TZ06KTH2UE9 11	PAINTED (red)
TRZ032	TZ06KTH2UE9 20	COMMON WARE
TRZ033	TZ06KTH2UE9 13	COMMON WARE
TRZ034	TZ06KTH2UE1 6	COMMON WARE
TRZ035	TZ06KTH2UE11 6	COMMON WARE
TRZ036	TZ06KTH2UE9 12	PAINTED (red)
TRZ037	TZ06KTH2UE12 2	COMMON WARE
TRZ038	TZ06KTH2UE1 1	COMMON WARE
TRZ039	TZ06KTH2UE12 6	COMMON WARE
TRZ040	TZ06KTH2UE1 4	COMMON WARE
TRZ041	TZ06KTH2UE12 1	COMMON WARE
TRZ042	TZ06KTH2UE9 14	COMMON WARE
TRZ043	TZ06KTH2UE9 6	COMMON WARE
TRZ044	TZ06KTHP6E1	COMMON WARE
TRZ045	TZ06KTHP7D1	PAINTED (red)
TRZ046	TZ06KTHP8D1	PAINTED (red)
TRZ047	TZ06KTHP4E1	COMMON WARE
TRZ048	TZ06KTHP9F1	PAINTED (red)
TRZ049	TZ06KTHP12A1	PAINTED (red)
TRZ050	TZ06KTHP3E1	COMMON WARE

Table 1: Analysed individuals inventory

JEOL JSM-840study Scanning Electron Microscope (SEM) equipped with Secondary Electron (SE) detector and Energy Dispersive X-ray Micro Analyser (EDXA) was used for the study of the microstructure and the sinterisation state of the ceramics. The observations were preformed under vacuum at the external surface of the fresh fractures and the secondary electron image was taken at 2000x magnification. At some cases also X-ray microanalysis was preformed. The acceleration voltage was

equal to 20kV and the intensity to $3x10^{-9}$ A. The preparation of the samples has been done by fixing the fresh fractures upon a standard metallic base of 1cm diameter with silicon and in order to insure the continuous conductivity between the sample and its base and to avoid the overloading of the surface of the fresh fractures were covered with silver and then the whole sample was covered carbon.

Chemical results

The raw chemical composition of the analysed ceramic material can be seen in Table 2. One of the most important steps in a chemical analysis, as it aims to compare the composition of the individuals analysed is to calculate somehow the variability in the data set. One of the simplest way to do that is to calculate the Compositional Variation Matrix (CVM) (Buxeda i Kilikoglou, 2003). This matrix includes all the necessary information to identify the variability in the data set, like the total variation and the variability that each element is introducing in the data set. Beside the above mentioned, it also indicates the relation between all the pair of elements. The CVM calculated for our data set can be seen in Table 3. It has been calculated without considering the following elements: Mo, Sn, Co, W, P_2O_5 and Pb. The first two elements have been left out because of the analytical imprecision, as both of them are under their regression limits in ceramics. The second two elements have been left out from the calculation, because they can be contaminated due to the sample preparation process and, the last two because they are elements which are very susceptible to suffer postdepositional contaminations, therefore they can introduce a false high variability in the data set. The total variation (vt) in this data set according to the CVM is very low (0.1684) which generally indicates a homogeneous composition and a monogenic character. At the first site the variability introduced by all the elements is relatively low. The mayor part of variability is introduced by the Ba. Looking at the chemical data there are two individuals with a very high Ba content (925 and 789 ppm) respect to the rest of the individuals which Ba content is approximately between 400 and 600 ppm. Therefore grate part of the variability introduced by this element in the data set is owed to these two individuals and it is probably a result of some kind of postdepositional contamination and/or alteration. Other elements which are affecting the variability more than the rest are: MgO, CaO, K_2O, Sr, Ce and Cu. However, the variability introduced by these elements can not be considered important.

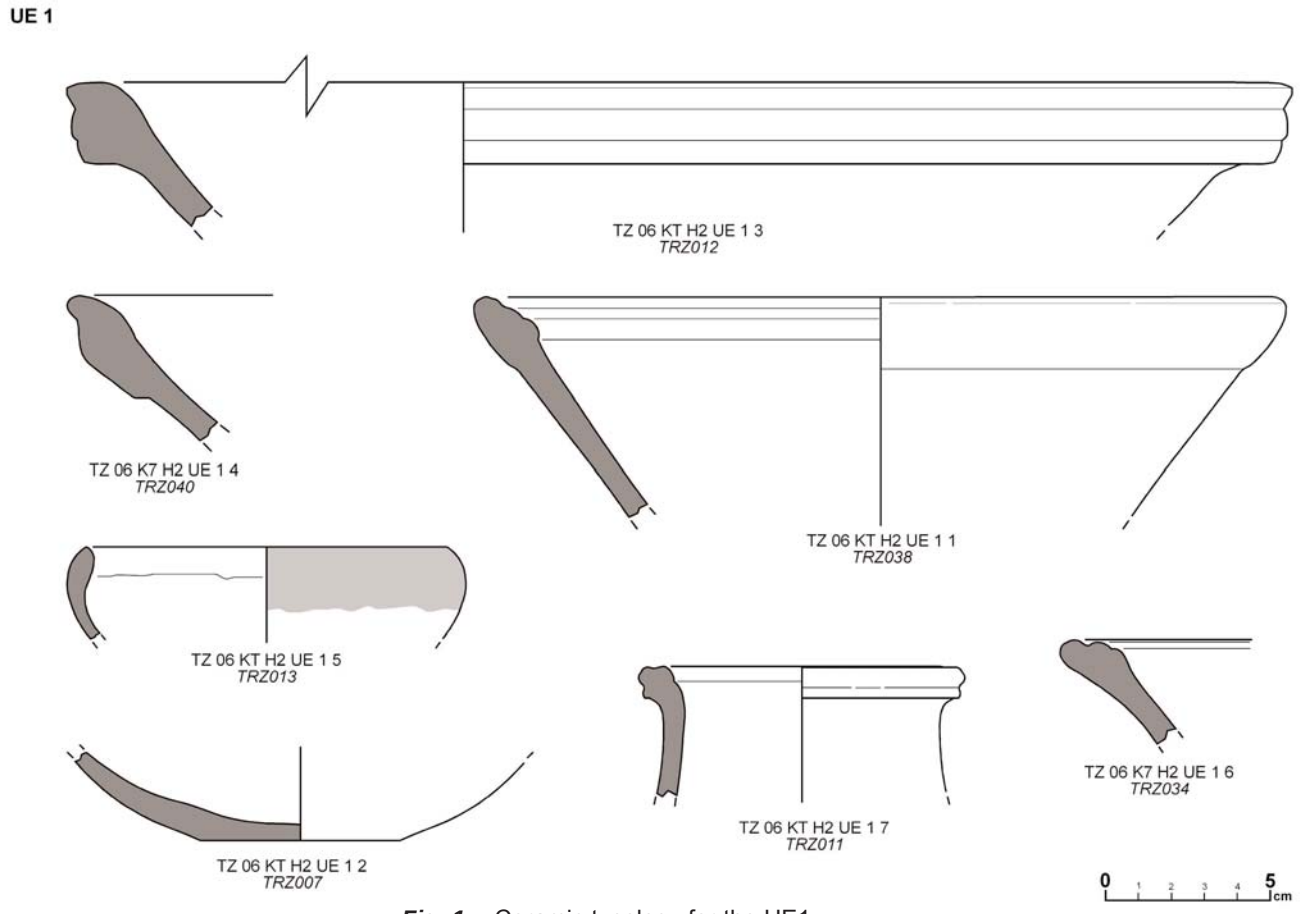

Fig. 1: . Ceramic typology for the UE1.

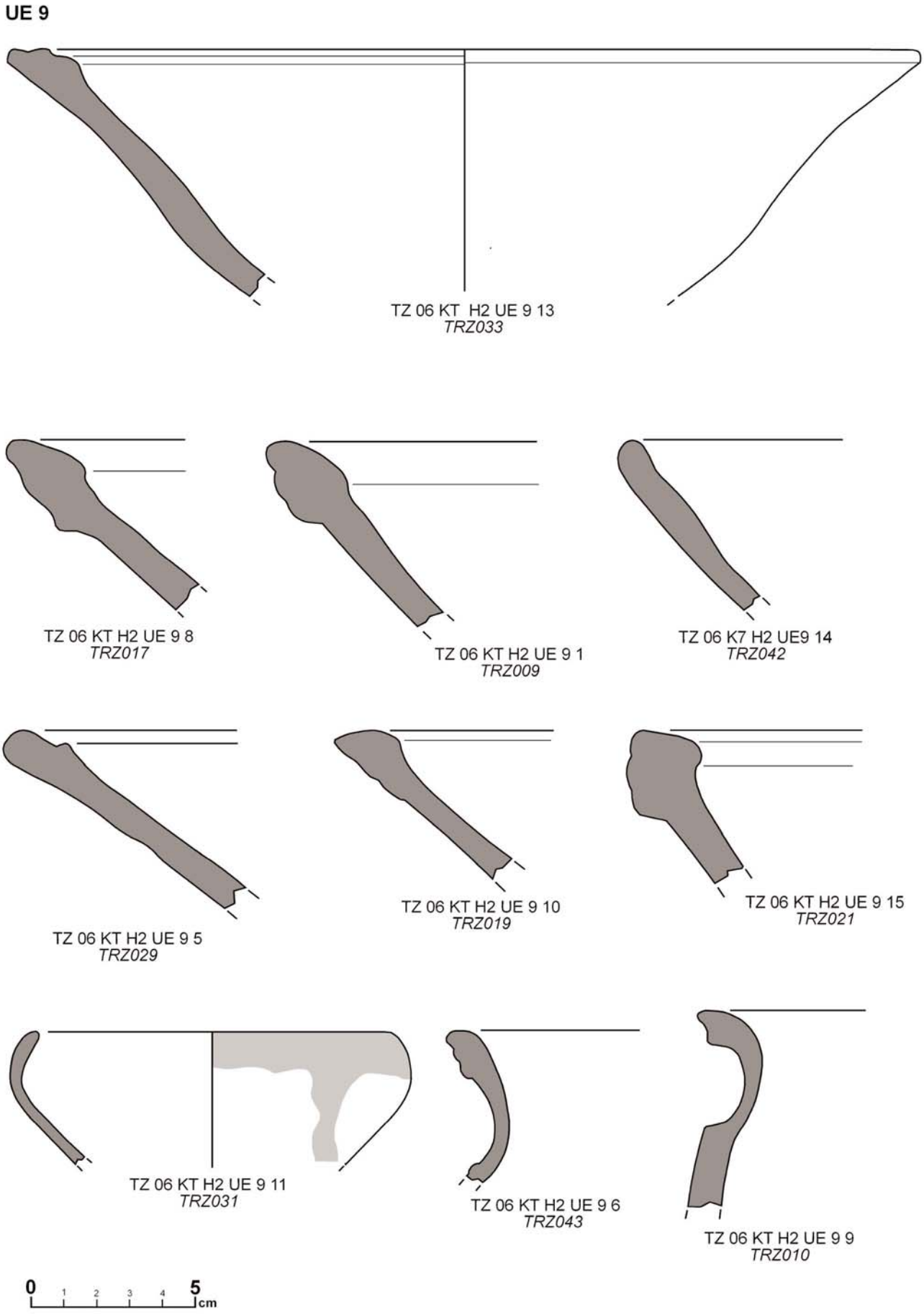

Fig. 2: . Ceramic typology for the UE9.

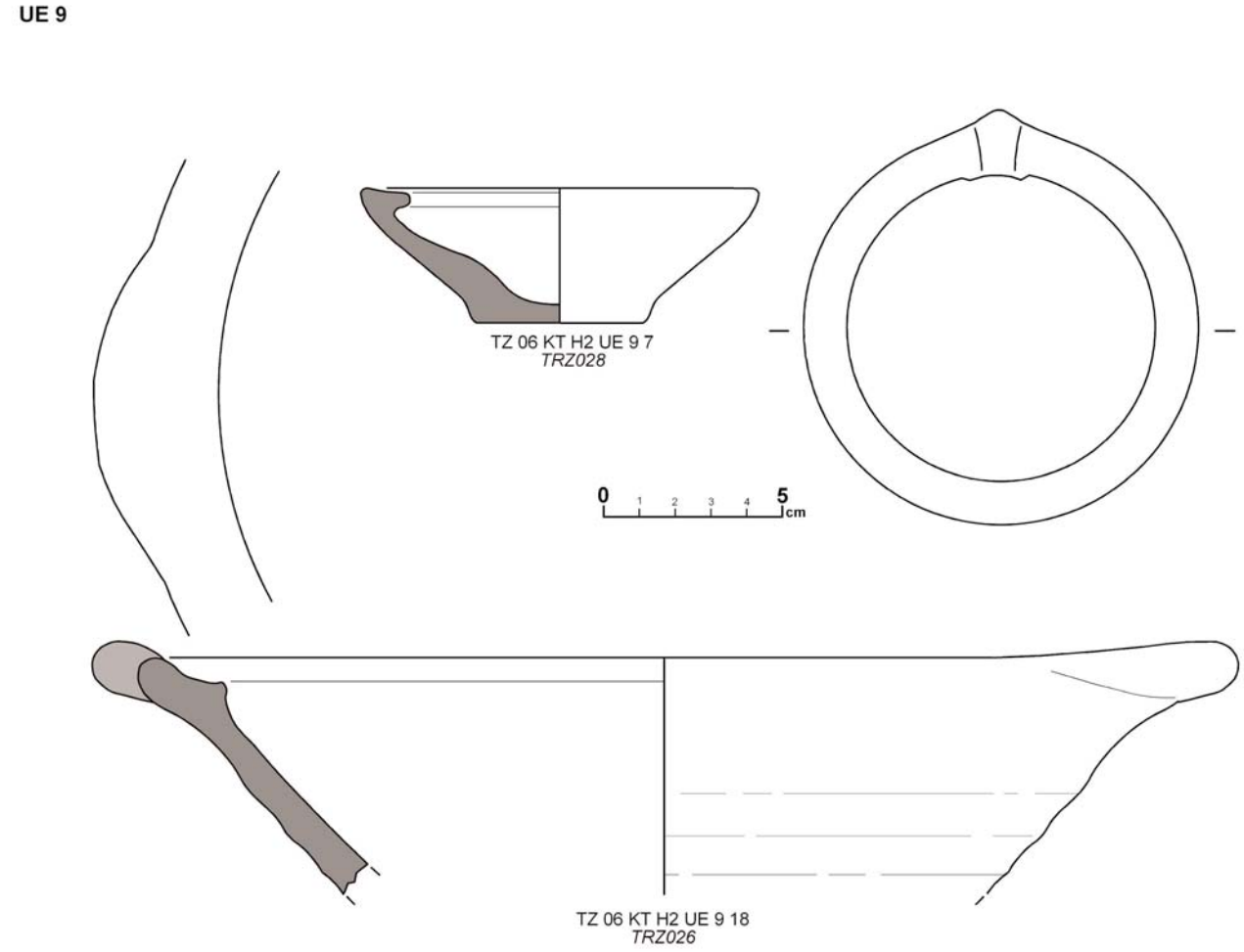

Fig. 3: . Ceramic typology for the UE9.

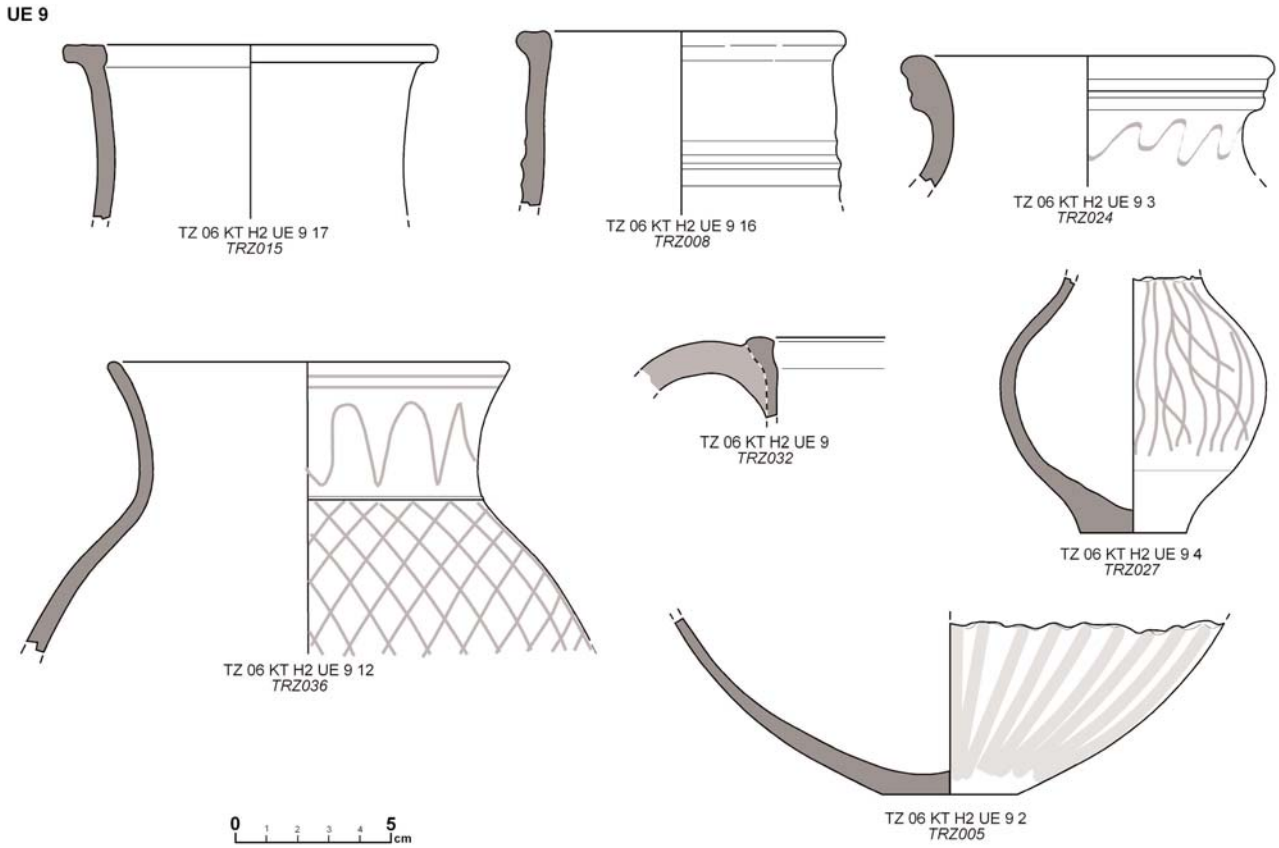

Fig. 4: . Ceramic typology for the UE9.

UE 11

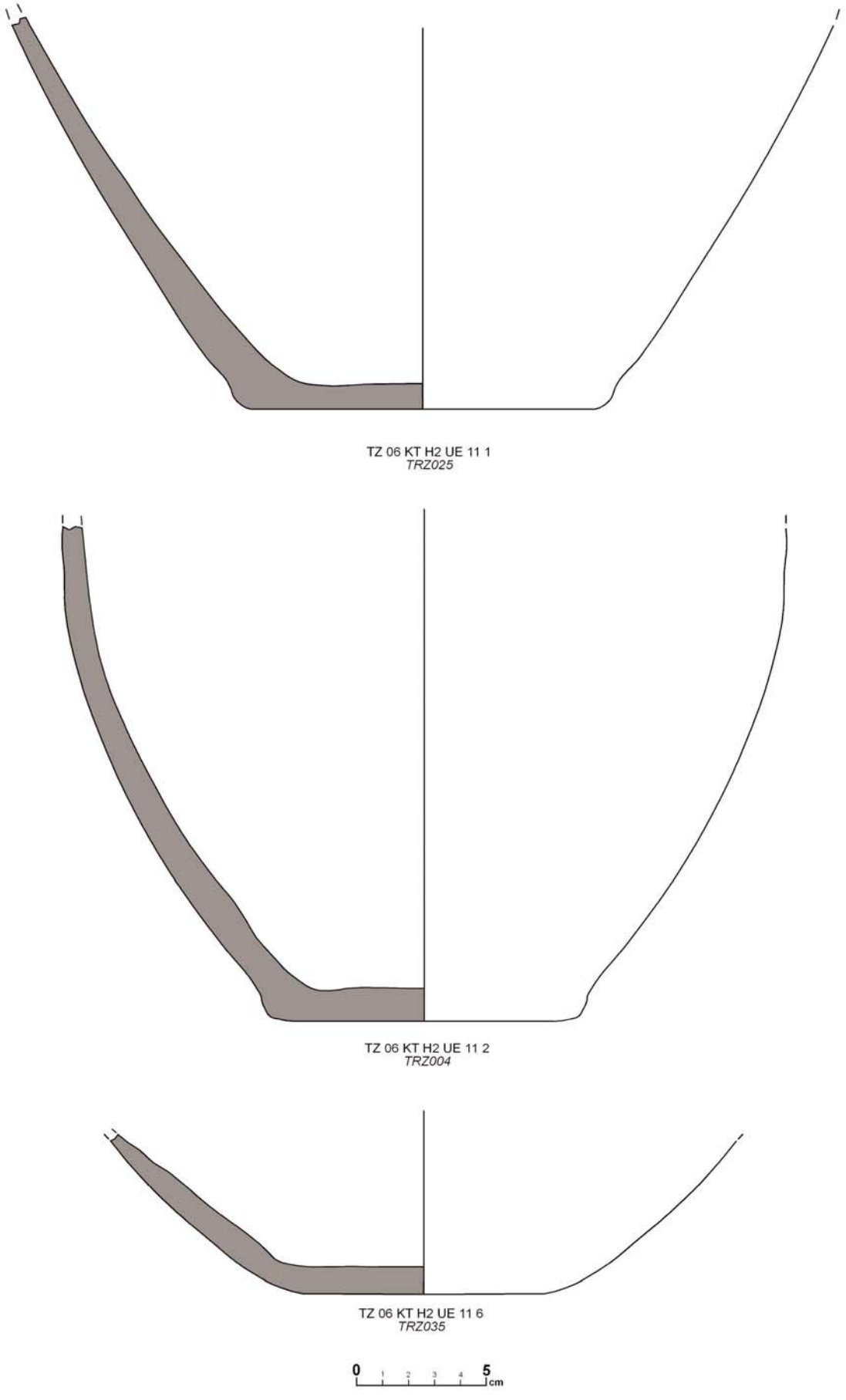

Fig. 5: . Ceramic typology for the UE11.

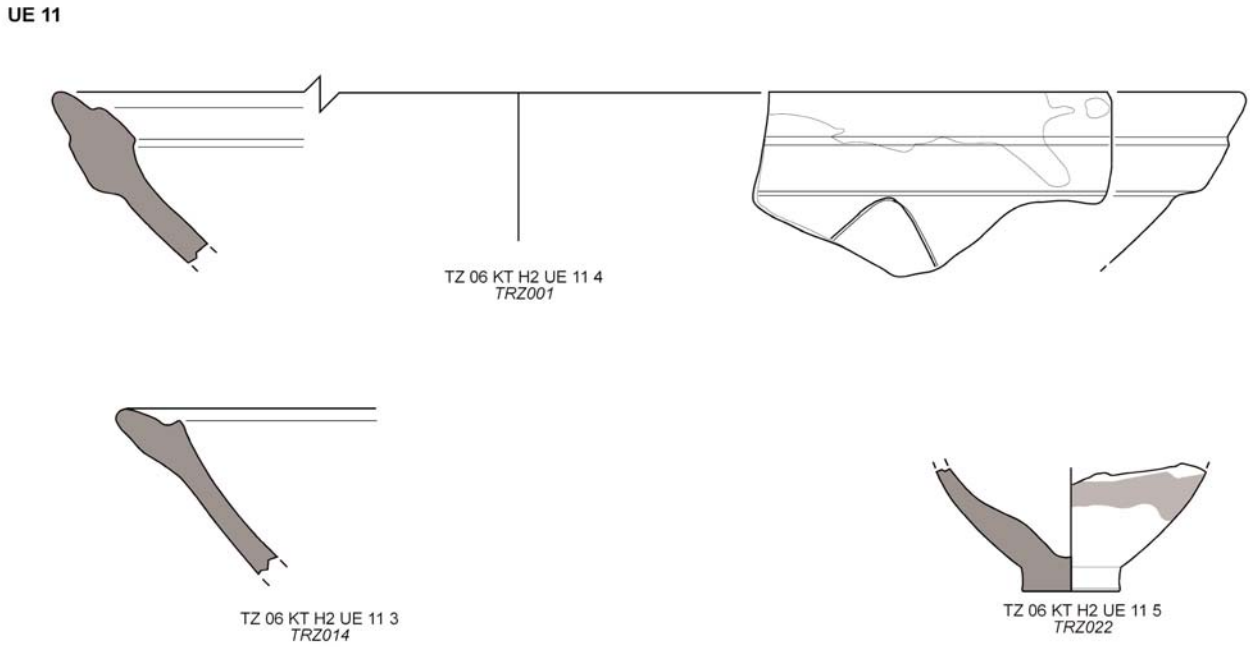

Fig. 6: . Ceramic typology for the UE11.

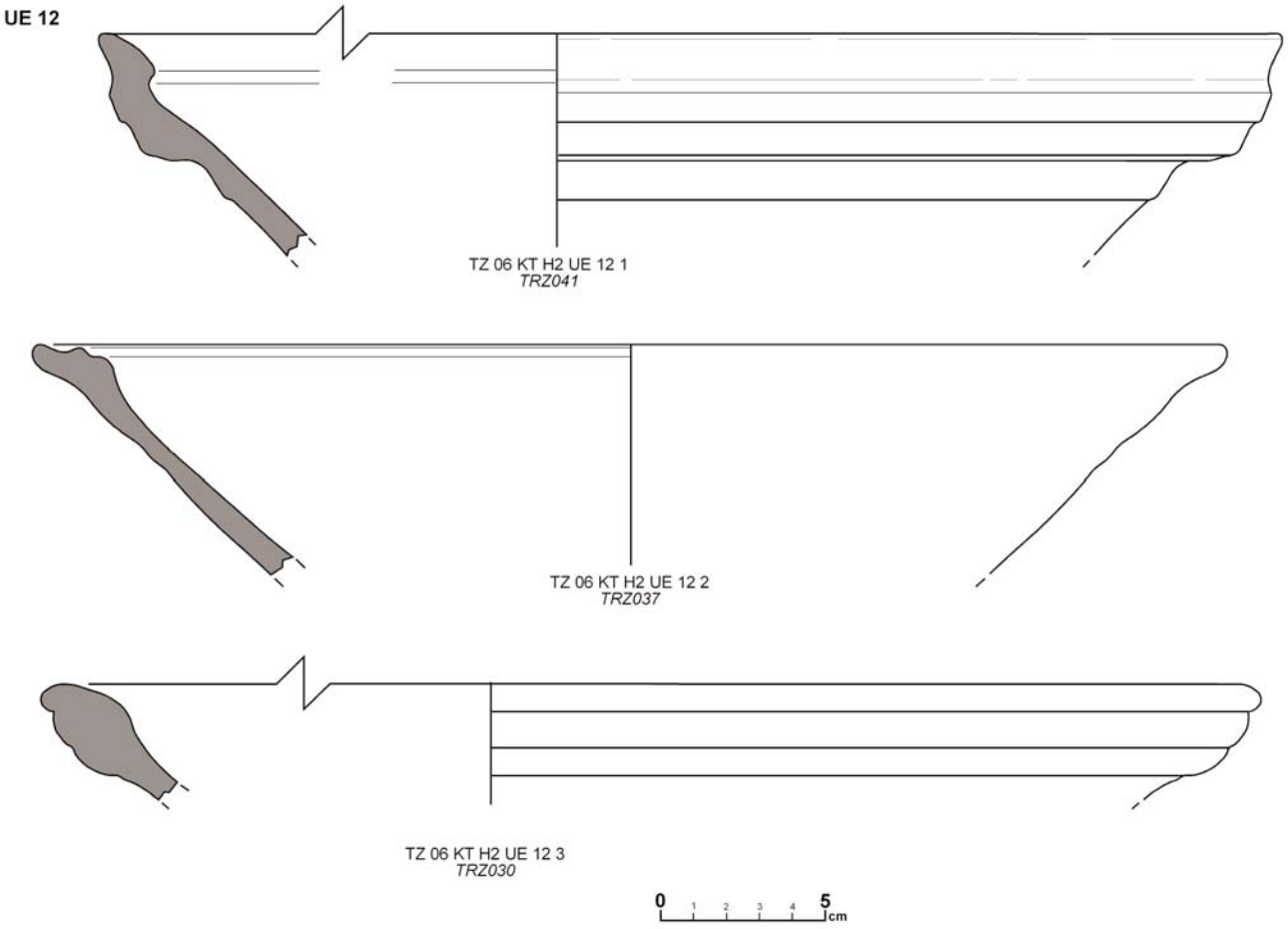

Fig. 7: . Ceramic typology for the UE12.

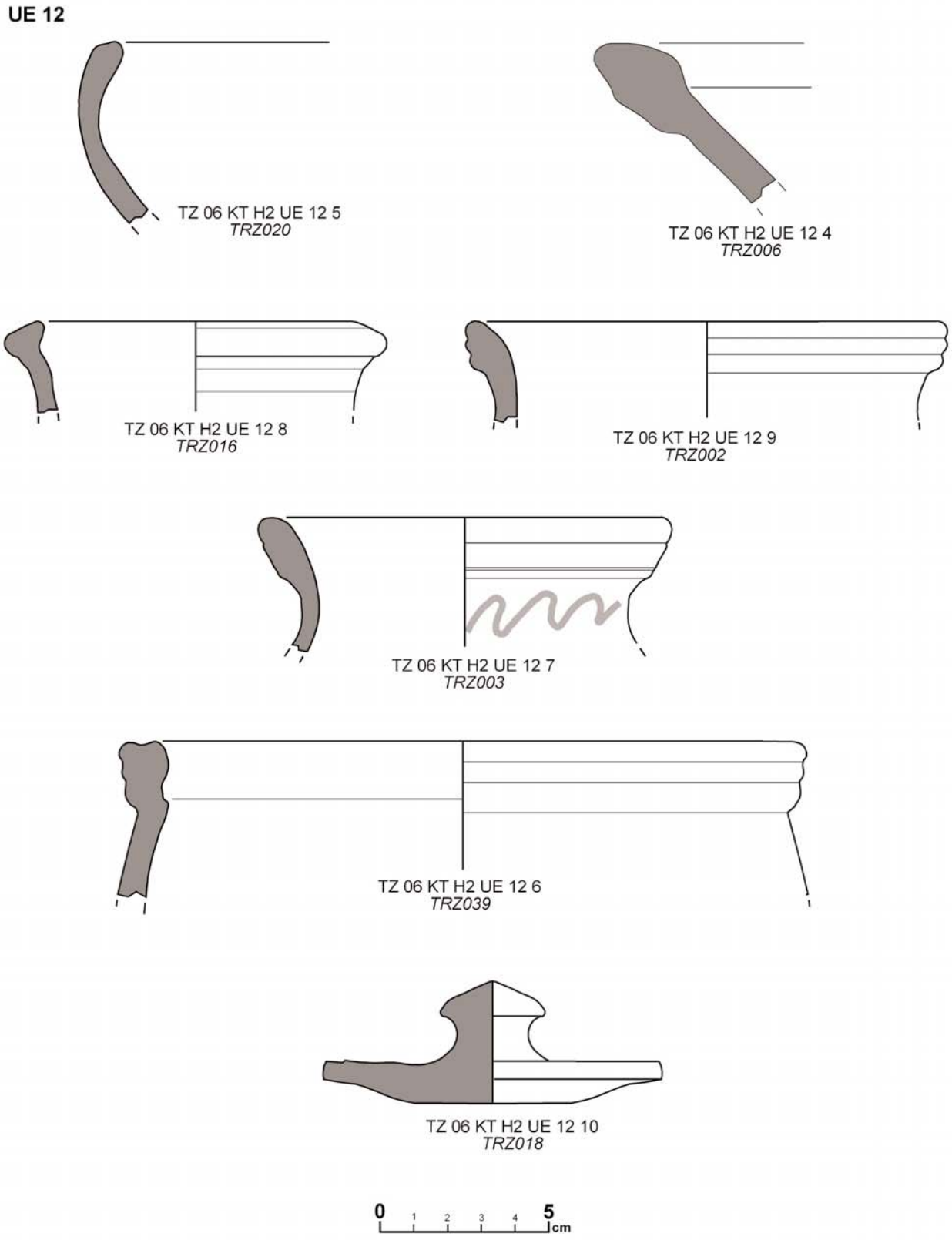

Fig. 8: . Ceramic typology for the UE12.

	Fe2O3	Al2O3	MnO	P2O5	TiO2	MgO	CaO	Na2O	K2O	SiO2	Ba	Rb	Mo	Th	Nb
TRZ001	5,41	14,51	0,09	0,29	0,59	4,06	10,47	2,05	3,24	54,98	0,0496	0,0122	0,0002	0,0016	0,0015
TRZ002	6,23	16,01	0,11	0,19	0,62	3,86	9,41	1,62	3,30	55,93	0,0569	0,0130	0,0002	0,0015	0,0016
TRZ003	5,67	15,01	0,09	0,25	0,62	4,06	10,13	1,62	3,39	55,24	0,0465	0,0124	0,0002	0,0014	0,0016
TRZ004	6,16	15,93	0,09	0,35	0,67	3,92	8,47	1,81	3,80	55,98	0,0522	0,0136	0,0001	0,0016	0,0016
TRZ005	5,97	15,34	0,09	0,24	0,66	3,82	10,10	1,46	3,42	53,80	0,0398	0,0121	0,0002	0,0014	0,0015
TRZ006	5,77	14,79	0,09	0,21	0,63	4,46	10,21	1,46	3,28	52,98	0,0444	0,0120	0,0002	0,0015	0,0015
TRZ008	5,98	15,73	0,09	0,22	0,67	3,35	7,98	1,74	3,80	58,40	0,0474	0,0123	0,0001	0,0014	0,0015
TRZ009	5,57	14,35	0,10	0,27	0,60	3,65	10,96	1,63	3,03	55,36	0,0503	0,0119	0,0001	0,0016	0,0015
TRZ010	5,63	15,13	0,09	0,23	0,59	3,86	10,20	1,41	3,27	55,32	0,0473	0,0124	0,0002	0,0016	0,0015
TRZ011	5,46	14,47	0,09	0,31	0,61	4,41	12,60	1,19	3,29	52,58	0,0458	0,0090	0,0001	0,0014	0,0014
TRZ012	6,03	15,37	0,10	0,25	0,62	3,69	10,75	1,28	3,23	54,72	0,0793	0,0123	0,0001	0,0014	0,0016
TRZ013	5,82	14,93	0,10	0,24	0,63	4,11	11,17	1,25	3,23	53,97	0,0578	0,0125	0,0001	0,0014	0,0015
TRZ014	5,52	14,67	0,09	0,22	0,59	3,74	12,57	1,31	3,27	52,97	0,0446	0,0121	0,0002	0,0015	0,0015
TRZ015	5,28	13,74	0,09	0,23	0,61	4,28	9,96	1,89	3,09	53,51	0,0472	0,0109	0,0002	0,0014	0,0015
TRZ016	5,87	14,90	0,10	0,20	0,64	4,13	11,50	2,02	3,33	53,61	0,0487	0,0102	0,0002	0,0013	0,0015
TRZ017	6,35	16,40	0,10	0,22	0,65	4,23	10,73	1,25	3,39	52,55	0,0513	0,0138	0,0001	0,0017	0,0015
TRZ018	5,73	15,33	0,10	0,25	0,65	3,46	8,13	1,92	3,43	58,03	0,0510	0,0124	0,0001	0,0016	0,0016
TRZ019	5,65	14,76	0,09	0,21	0,61	3,99	11,44	1,78	3,37	52,86	0,0470	0,0123	0,0002	0,0015	0,0015
TRZ020	5,92	15,25	0,10	0,26	0,68	3,75	10,35	2,02	2,64	56,58	0,0517	0,0103	0,0001	0,0016	0,0017
TRZ021	5,68	14,95	0,10	0,19	0,61	3,95	10,34	1,78	3,06	54,39	0,0477	0,0120	0,0002	0,0013	0,0015
TRZ022	5,69	14,97	0,09	0,28	0,61	3,81	11,31	1,47	3,38	53,25	0,0457	0,0123	0,0001	0,0015	0,0015
TRZ023	5,78	15,01	0,10	0,26	0,63	4,17	10,21	1,46	3,34	54,22	0,0477	0,0125	0,0003	0,0016	0,0015
TRZ024	5,64	14,86	0,09	0,24	0,61	4,00	11,57	1,45	3,28	53,75	0,0451	0,0121	0,0001	0,0013	0,0015
TRZ025	5,55	14,44	0,09	0,27	0,62	3,87	10,53	2,26	3,57	52,75	0,0464	0,0118	0,0001	0,0015	0,0015
TRZ026	5,85	15,24	0,09	0,36	0,63	4,15	12,03	1,49	3,11	53,76	0,0470	0,0116	0,0001	0,0016	0,0015
TRZ027	6,20	16,20	0,09	0,61	0,65	4,04	9,34	1,48	3,90	54,95	0,0489	0,0131	0,0001	0,0015	0,0015
TRZ028	6,14	15,43	0,11	0,18	0,68	3,91	10,79	2,23	2,27	55,94	0,0440	0,0084	0,0001	0,0013	0,0016
TRZ029	5,47	14,35	0,09	0,30	0,59	3,96	12,17	1,14	3,18	52,60	0,0447	0,0118	0,0001	0,0013	0,0015
TRZ030	5,70	14,69	0,10	0,22	0,64	4,16	12,08	1,58	2,84	53,56	0,0452	0,0110	0,0001	0,0016	0,0015
TRZ031	5,86	15,34	0,09	0,25	0,63	4,08	10,86	1,48	3,34	54,41	0,0462	0,0125	0,0001	0,0015	0,0016
TRZ032	5,61	14,98	0,09	0,22	0,59	3,92	11,20	1,52	3,21	53,85	0,0454	0,0124	0,0001	0,0017	0,0015
TRZ033	5,52	14,50	0,10	0,21	0,63	3,53	11,20	1,69	2,90	55,44	0,0470	0,0101	0,0001	0,0014	0,0015
TRZ034	5,88	15,13	0,10	0,32	0,65	3,72	10,72	1,36	3,26	53,48	0,0563	0,0117	0,0002	0,0015	0,0016
TRZ035	5,69	14,74	0,11	0,26	0,62	3,74	10,46	1,89	3,45	53,89	0,0522	0,0123	0,0002	0,0015	0,0015
TRZ036	5,85	15,32	0,09	0,40	0,63	3,70	8,80	1,51	3,74	54,65	0,0455	0,0127	0,0001	0,0015	0,0015
TRZ037	5,63	14,84	0,09	0,25	0,61	4,09	11,79	1,59	2,94	54,07	0,0495	0,0111	0,0001	0,0014	0,0016
TRZ038	5,52	14,37	0,10	0,25	0,65	3,45	11,30	1,32	3,05	54,89	0,0552	0,0112	0,0001	0,0014	0,0015
TRZ039	5,52	14,45	0,09	0,31	0,60	3,17	9,89	1,62	3,59	54,40	0,0529	0,0117	0,0003	0,0014	0,0015
TRZ040	5,75	15,02	0,09	0,28	0,63	4,32	11,13	1,35	2,99	55,24	0,0533	0,0111	0,0001	0,0015	0,0016
TRZ041	5,83	15,24	0,09	0,21	0,62	4,22	10,17	1,27	3,15	53,96	0,0462	0,0122	0,0002	0,0014	0,0015
TRZ042	5,07	13,58	0,12	0,22	0,56	3,17	10,43	1,68	3,18	54,53	0,0452	0,0109	0,0002	0,0013	0,0014
TRZ043	5,81	15,16	0,09	0,26	0,61	4,40	10,94	1,29	3,36	52,83	0,0446	0,0124	0,0002	0,0015	0,0016
TRZ044	5,39	14,71	0,09	0,35	0,60	3,44	9,64	1,33	3,09	57,10	0,0678	0,0118	0,0001	0,0014	0,0015
TRZ045	5,42	14,43	0,10	0,25	0,63	3,72	10,34	1,27	3,03	56,32	0,0582	0,0111	0,0001	0,0014	0,0015
TRZ046	5,43	14,16	0,10	0,24	0,62	4,03	10,69	1,39	2,87	55,11	0,0576	0,0104	0,0001	0,0014	0,0015
TRZ047	6,10	15,64	0,10	0,32	0,64	4,01	11,55	1,25	3,04	53,74	0,0671	0,0128	0,0001	0,0016	0,0016
TRZ048	5,84	15,17	0,10	0,25	0,64	3,50	9,72	1,21	3,26	56,17	0,0493	0,0119	0,0002	0,0016	0,0015
TRZ049	5,77	14,85	0,11	0,19	0,62	3,24	11,04	1,07	3,09	54,68	0,0748	0,0120	0,0002	0,0015	0,0015
TRZ050	5,05	13,48	0,09	0,22	0,60	3,27	9,05	1,03	2,97	55,99	0,0851	0,0102	0,0000	0,0013	0,0015

Table. 2.1: . Normalized chemical data.

	Pb	Zr	Y	Sr	Sn	Ce	Co	Ga	V	Zn	W	Cu	Ni	Cr	loi
TRZ001	0,0023	0,0145	0,0027	0,0380	0,0001	0,0060	0,0098	0,0021	0,0091	0,0102	0,0495	0,0034	0,0047	0,0077	4,4747
TRZ002	0,0019	0,0149	0,0027	0,0311	0,0002	0,0061	0,0105	0,0023	0,0102	0,0112	0,0680	0,0036	0,0050	0,0077	2,7532
TRZ003	0,0019	0,0145	0,0028	0,0371	0,0001	0,0053	0,0060	0,0022	0,0101	0,0109	0,0398	0,0034	0,0048	0,0078	4,1722
TRZ004	0,0020	0,0152	0,0029	0,0377	0,0003	0,0070	0,0061	0,0023	0,0108	0,0096	0,0331	0,0036	0,0054	0,0081	2,7276
TRZ005	0,0022	0,0144	0,0028	0,0319	0,0003	0,0059	0,0046	0,0021	0,0098	0,0101	0,0258	0,0029	0,0045	0,0079	5,2597
TRZ006	0,0023	0,0150	0,0027	0,0370	0,0004	0,0055	0,0042	0,0021	0,0097	0,0100	0,0202	0,0033	0,0047	0,0077	6,0405
TRZ008	0,0013	0,0144	0,0028	0,0270	0,0002	0,0050	0,0069	0,0021	0,0106	0,0079	0,0413	0,0029	0,0048	0,0081	2,5902
TRZ009	0,0018	0,0153	0,0027	0,0366	0,0001	0,0050	0,0061	0,0020	0,0089	0,0103	0,0430	0,0035	0,0045	0,0074	4,3156
TRZ010	0,0024	0,0139	0,0026	0,0312	0,0002	0,0058	0,0057	0,0021	0,0099	0,0102	0,0390	0,0030	0,0048	0,0076	4,4957
TRZ011	0,0011	0,0133	0,0027	0,0462	0,0001	0,0040	0,0180	0,0020	0,0095	0,0101	0,0320	0,0033	0,0040	0,0068	4,7783
TRZ012	0,0015	0,0145	0,0028	0,0427	0,0004	0,0062	0,0065	0,0023	0,0102	0,0104	0,0367	0,0042	0,0054	0,0076	3,4197
TRZ013	0,0015	0,0153	0,0028	0,0378	0,0002	0,0069	0,0053	0,0022	0,0098	0,0112	0,0304	0,0036	0,0049	0,0075	4,2272
TRZ014	0,0016	0,0144	0,0027	0,0363	0,0004	0,0067	0,0047	0,0021	0,0093	0,0105	0,0249	0,0031	0,0049	0,0075	5,0956
TRZ015	0,0007	0,0155	0,0028	0,0385	0,0000	0,0065	0,0045	0,0020	0,0101	0,0100	0,0220	0,0030	0,0044	0,0074	6,9919
TRZ016	0,0009	0,0154	0,0029	0,0396	0,0004	0,0056	0,0058	0,0021	0,0098	0,0098	0,0328	0,0037	0,0053	0,0076	3,0303
TRZ017	0,0012	0,0144	0,0029	0,0345	0,0003	0,0068	0,0043	0,0024	0,0108	0,0115	0,0228	0,0040	0,0053	0,0078	3,4767
TRZ018	0,0024	0,0163	0,0029	0,0327	0,0002	0,0071	0,0065	0,0021	0,0098	0,0097	0,0465	0,0031	0,0047	0,0075	3,5058
TRZ019	0,0014	0,0138	0,0027	0,0359	0,0003	0,0042	0,0043	0,0021	0,0101	0,0105	0,0250	0,0031	0,0049	0,0074	5,506
TRZ020	0,0015	0,0166	0,0031	0,0321	0,0001	0,0064	0,0054	0,0022	0,0101	0,0110	0,0371	0,0041	0,0048	0,0079	1,6446
TRZ021	0,0017	0,0147	0,0028	0,0335	0,0001	0,0050	0,0048	0,0021	0,0097	0,0102	0,0343	0,0038	0,0047	0,0074	4,5293
TRZ022	0,0026	0,0144	0,0027	0,0359	0,0001	0,0055	0,0039	0,0020	0,0094	0,0103	0,0192	0,0032	0,0048	0,0074	5,263
TRZ023	0,0026	0,0143	0,0028	0,0426	0,0001	0,0063	0,0041	0,0021	0,0102	0,0104	0,0216	0,0032	0,0050	0,0079	4,7826
TRZ024	0,0020	0,0138	0,0027	0,0372	0,0004	0,0062	0,0041	0,0020	0,0102	0,0106	0,0224	0,0030	0,0051	0,0078	4,9968
TRZ025	0,0022	0,0141	0,0028	0,0388	0,0002	0,0068	0,0036	0,0021	0,0092	0,0101	0,0139	0,0029	0,0046	0,0073	7,0903
TRZ026	0,0014	0,0145	0,0028	0,0382	0,0003	0,0057	0,0055	0,0021	0,0100	0,0109	0,0311	0,0033	0,0051	0,0079	3,4646
TRZ027	0,0023	0,0140	0,0029	0,0421	0,0004	0,0043	0,0033	0,0022	0,0118	0,0091	0,0159	0,0027	0,0054	0,0083	2,7151
TRZ028	0,0017	0,0161	0,0029	0,0331	0,0002	0,0057	0,0052	0,0022	0,0096	0,0097	0,0338	0,0037	0,0050	0,0079	1,754
TRZ029	0,0017	0,0138	0,0027	0,0435	0,0002	0,0046	0,0037	0,0020	0,0093	0,0101	0,0216	0,0034	0,0047	0,0073	5,4705
TRZ030	0,0018	0,0152	0,0029	0,0350	0,0000	0,0059	0,0047	0,0021	0,0096	0,0102	0,0280	0,0035	0,0050	0,0075	3,7579
TRZ031	0,0018	0,0147	0,0028	0,0356	0,0001	0,0070	0,0126	0,0022	0,0103	0,0118	0,0389	0,0033	0,0047	0,0077	3,1735
TRZ032	0,0011	0,0139	0,0026	0,0325	0,0001	0,0054	0,0068	0,0021	0,0098	0,0108	0,0481	0,0030	0,0048	0,0078	3,5902
TRZ033	0,0014	0,0151	0,0028	0,0344	0,0003	0,0062	0,0057	0,0020	0,0093	0,0101	0,0348	0,0032	0,0044	0,0077	3,73
TRZ034	0,0022	0,0153	0,0029	0,0391	0,0001	0,0066	0,0054	0,0022	0,0091	0,0108	0,0305	0,0032	0,0048	0,0078	2,6885
TRZ035	0,0022	0,0142	0,0027	0,0386	0,0003	0,0062	0,0043	0,0021	0,0102	0,0100	0,0228	0,0028	0,0049	0,0075	4,6782
TRZ036	0,0026	0,0146	0,0027	0,0370	0,0003	0,0062	0,0044	0,0021	0,0100	0,0100	0,0233	0,0031	0,0050	0,0079	3,8591
TRZ037	0,0007	0,0145	0,0027	0,0378	0,0001	0,0071	0,0053	0,0021	0,0099	0,0105	0,0333	0,0034	0,0050	0,0082	2,9811
TRZ038	0,0021	0,0158	0,0029	0,0396	0,0003	0,0058	0,0057	0,0020	0,0093	0,0101	0,0407	0,0043	0,0045	0,0076	4,3944
TRZ039	0,0024	0,0149	0,0028	0,0320	0,0001	0,0071	0,0039	0,0021	0,0097	0,0101	0,0207	0,0030	0,0044	0,0074	8,8155
TRZ040	0,0011	0,0152	0,0028	0,0405	0,0004	0,0065	0,0055	0,0021	0,0102	0,0107	0,0336	0,0038	0,0049	0,0076	2,1256
TRZ041	0,0023	0,0146	0,0026	0,0304	0,0001	0,0039	0,0051	0,0021	0,0092	0,0103	0,0320	0,0032	0,0050	0,0083	4,4851
TRZ042	0,0025	0,0140	0,0025	0,0335	0,0001	0,0065	0,0043	0,0019	0,0088	0,0088	0,0273	0,0027	0,0041	0,0068	7,5804
TRZ043	0,0025	0,0138	0,0027	0,0377	0,0001	0,0065	0,0047	0,0022	0,0092	0,0103	0,0223	0,0035	0,0051	0,0083	4,9585
TRZ044	0,0016	0,0146	0,0026	0,0375	0,0000	0,0052	0,0064	0,0021	0,0092	0,0096	0,0415	0,0034	0,0043	0,0077	3,1186
TRZ045	0,0012	0,0154	0,0027	0,0396	0,0001	0,0053	0,0052	0,0020	0,0095	0,0095	0,0322	0,0039	0,0043	0,0076	3,2734
TRZ046	0,0011	0,0159	0,0027	0,0404	0,0000	0,0068	0,0061	0,0020	0,0097	0,0098	0,0379	0,0039	0,0046	0,0076	3,2354
TRZ047	0,0026	0,0147	0,0027	0,0375	0,0004	0,0055	0,0048	0,0022	0,0107	0,0114	0,0271	0,0041	0,0051	0,0076	3,0939
TRZ048	0,0027	0,0145	0,0027	0,0345	0,0004	0,0055	0,0057	0,0021	0,0099	0,0093	0,0352	0,0029	0,0048	0,0076	3,6684
TRZ049	0,0024	0,0146	0,0027	0,0376	0,0001	0,0040	0,0044	0,0021	0,0102	0,0095	0,0231	0,0039	0,0050	0,0070	4,7605
TRZ050	0,0023	0,0152	0,0027	0,0449	0,0003	0,0059	0,0043	0,0018	0,0091	0,0089	0,0218	0,0028	0,0040	0,0068	8,016

Table 2.2: . Normalized chemical data.

elements	Fe2O3	Al2O3	MnO	TiO2	MgO	CaO	Na2O	K2O	SiO2	Ba	Rb	Th
Fe2O3	0,0000	0,0003	0,0072	0,0012	0,0074	0,0144	0,0354	0,0092	0,0029	0,0280	0,0078	0,0052
Al2O3	0,0003	0,0000	0,0073	0,0013	0,0074	0,0141	0,0355	0,0079	0,0020	0,0274	0,0068	0,0046
MnO	0,0072	0,0073	0,0000	0,0064	0,0175	0,0155	0,0369	0,0192	0,0054	0,0241	0,0174	0,0119
TiO2	0,0012	0,0013	0,0064	0,0000	0,0085	0,0146	0,0331	0,0106	0,0016	0,0264	0,0110	0,0062
MgO	0,0074	0,0074	0,0175	0,0085	0,0000	0,0112	0,0407	0,0168	0,0106	0,0433	0,0159	0,0108
CaO	0,0144	0,0141	0,0155	0,0146	0,0112	0,0000	0,0533	0,0268	0,0146	0,0400	0,0254	0,0170
Na2O	0,0354	0,0355	0,0369	0,0331	0,0407	0,0533	0,0000	0,0439	0,0335	0,0840	0,0488	0,0391
K2O	0,0092	0,0079	0,0192	0,0106	0,0168	0,0268	0,0439	0,0000	0,0097	0,0377	0,0054	0,0114
SiO2	0,0029	0,0020	0,0054	0,0016	0,0106	0,0146	0,0335	0,0097	0,0000	0,0227	0,0100	0,0063
Ba	0,0280	0,0274	0,0241	0,0264	0,0433	0,0400	0,0840	0,0377	0,0227	0,0000	0,0331	0,0317
Rb	0,0078	0,0068	0,0174	0,0110	0,0159	0,0254	0,0488	0,0054	0,0100	0,0331	0,0000	0,0077
Th	0,0052	0,0046	0,0119	0,0062	0,0108	0,0170	0,0391	0,0114	0,0063	0,0317	0,0077	0,0000
Nb	0,0019	0,0016	0,0067	0,0015	0,0081	0,0130	0,0332	0,0114	0,0014	0,0237	0,0096	0,0057
Zr	0,0043	0,0040	0,0054	0,0019	0,0112	0,0150	0,0321	0,0151	0,0017	0,0229	0,0142	0,0080
Y	0,0020	0,0020	0,0066	0,0007	0,0083	0,0128	0,0311	0,0107	0,0019	0,0264	0,0114	0,0063
Sr	0,0167	0,0161	0,0188	0,0146	0,0143	0,0145	0,0601	0,0204	0,0140	0,0246	0,0244	0,0197
Ce	0,0279	0,0274	0,0290	0,0260	0,0342	0,0400	0,0441	0,0343	0,0257	0,0503	0,0323	0,0278
Ga	0,0007	0,0007	0,0075	0,0022	0,0073	0,0141	0,0344	0,0093	0,0032	0,0270	0,0071	0,0048
V	0,0019	0,0017	0,0093	0,0026	0,0085	0,0168	0,0370	0,0081	0,0035	0,0267	0,0078	0,0063
Zn	0,0054	0,0052	0,0115	0,0069	0,0063	0,0081	0,0414	0,0158	0,0075	0,0316	0,0110	0,0069
Cu	0,0135	0,0144	0,0152	0,0133	0,0180	0,0179	0,0558	0,0336	0,0151	0,0248	0,0262	0,0194
Ni	0,0020	0,0025	0,0106	0,0045	0,0079	0,0151	0,0371	0,0111	0,0063	0,0311	0,0077	0,0070
Cr	0,0017	0,0013	0,0095	0,0019	0,0068	0,0147	0,0335	0,0095	0,0024	0,0310	0,0082	0,0060
t.i	0,1971	0,1914	0,2990	0,1970	0,3212	0,4289	0,9238	0,3780	0,2019	0,7183	0,3490	0,2697
vt/t.i	0,8545	0,8796	0,5632	0,8548	0,5241	0,3926	0,1823	0,4455	0,8339	0,2344	0,4825	0,6242
r v,t	0,9914	0,9911	0,9599	0,9920	0,9436	0,9233	0,8403	0,9206	0,9860	0,8655	0,9368	0,9849
vt	0,1684											

elements	Nb	Zr	Y	Sr	Ce	Ga	V	Zn	Cu	Ni	Cr
Fe2O3	0,0019	0,0043	0,0020	0,0167	0,0279	0,0007	0,0019	0,0054	0,0135	0,0020	0,0017
Al2O3	0,0016	0,0040	0,0020	0,0161	0,0274	0,0007	0,0017	0,0052	0,0144	0,0025	0,0013
MnO	0,0067	0,0054	0,0066	0,0188	0,0290	0,0075	0,0093	0,0115	0,0152	0,0106	0,0095
TiO2	0,0015	0,0019	0,0007	0,0146	0,0260	0,0022	0,0026	0,0069	0,0133	0,0045	0,0019
MgO	0,0081	0,0112	0,0083	0,0143	0,0342	0,0073	0,0085	0,0063	0,0180	0,0079	0,0068
CaO	0,0130	0,0150	0,0128	0,0145	0,0400	0,0141	0,0168	0,0081	0,0179	0,0151	0,0147
Na2O	0,0332	0,0321	0,0311	0,0601	0,0441	0,0344	0,0370	0,0414	0,0558	0,0371	0,0335
K2O	0,0114	0,0151	0,0107	0,0204	0,0343	0,0093	0,0081	0,0158	0,0336	0,0111	0,0095
SiO2	0,0014	0,0017	0,0019	0,0140	0,0257	0,0032	0,0035	0,0075	0,0151	0,0063	0,0024
Ba	0,0237	0,0229	0,0264	0,0246	0,0503	0,0270	0,0267	0,0316	0,0248	0,0311	0,0310
Rb	0,0096	0,0142	0,0114	0,0244	0,0323	0,0071	0,0078	0,0110	0,0262	0,0077	0,0082
Th	0,0057	0,0080	0,0063	0,0197	0,0278	0,0048	0,0063	0,0069	0,0194	0,0070	0,0060
Nb	0,0000	0,0020	0,0014	0,0138	0,0226	0,0017	0,0033	0,0044	0,0123	0,0042	0,0018
Zr	0,0020	0,0000	0,0017	0,0149	0,0224	0,0045	0,0058	0,0074	0,0118	0,0077	0,0040
Y	0,0014	0,0017	0,0000	0,0128	0,0237	0,0023	0,0031	0,0058	0,0130	0,0048	0,0026
Sr	0,0138	0,0149	0,0128	0,0000	0,0388	0,0165	0,0153	0,0158	0,0220	0,0179	0,0166
Ce	0,0226	0,0224	0,0237	0,0388	0,0000	0,0251	0,0292	0,0248	0,0394	0,0293	0,0258
Ga	0,0017	0,0045	0,0023	0,0165	0,0251	0,0000	0,0025	0,0043	0,0126	0,0025	0,0020
V	0,0033	0,0058	0,0031	0,0153	0,0292	0,0025	0,0000	0,0076	0,0169	0,0034	0,0033
Zn	0,0044	0,0074	0,0058	0,0158	0,0248	0,0043	0,0076	0,0000	0,0130	0,0072	0,0062
Cu	0,0123	0,0118	0,0130	0,0220	0,0394	0,0126	0,0169	0,0130	0,0000	0,0152	0,0159
Ni	0,0042	0,0077	0,0048	0,0179	0,0293	0,0025	0,0034	0,0072	0,0152	0,0000	0,0032
Cr	0,0018	0,0040	0,0026	0,0166	0,0258	0,0020	0,0033	0,0062	0,0159	0,0032	0,0000
t.i	0,1853	0,2181	0,1914	0,4427	0,6800	0,1923	0,2208	0,2542	0,4391	0,2381	0,2081
vt/t.i	0,9087	0,7719	0,8798	0,3804	0,2476	0,8756	0,7626	0,6624	0,3835	0,7072	0,8092
r v,t	0,9968	0,9689	0,9918	0,8770	0,8920	0,9919	0,9855	0,9639	0,8874	0,9842	0,9860
vt											

Table 3: . Compositional Variation Matrix without considering: Mo, Sn, Co, W, P_2O_5 and Pb

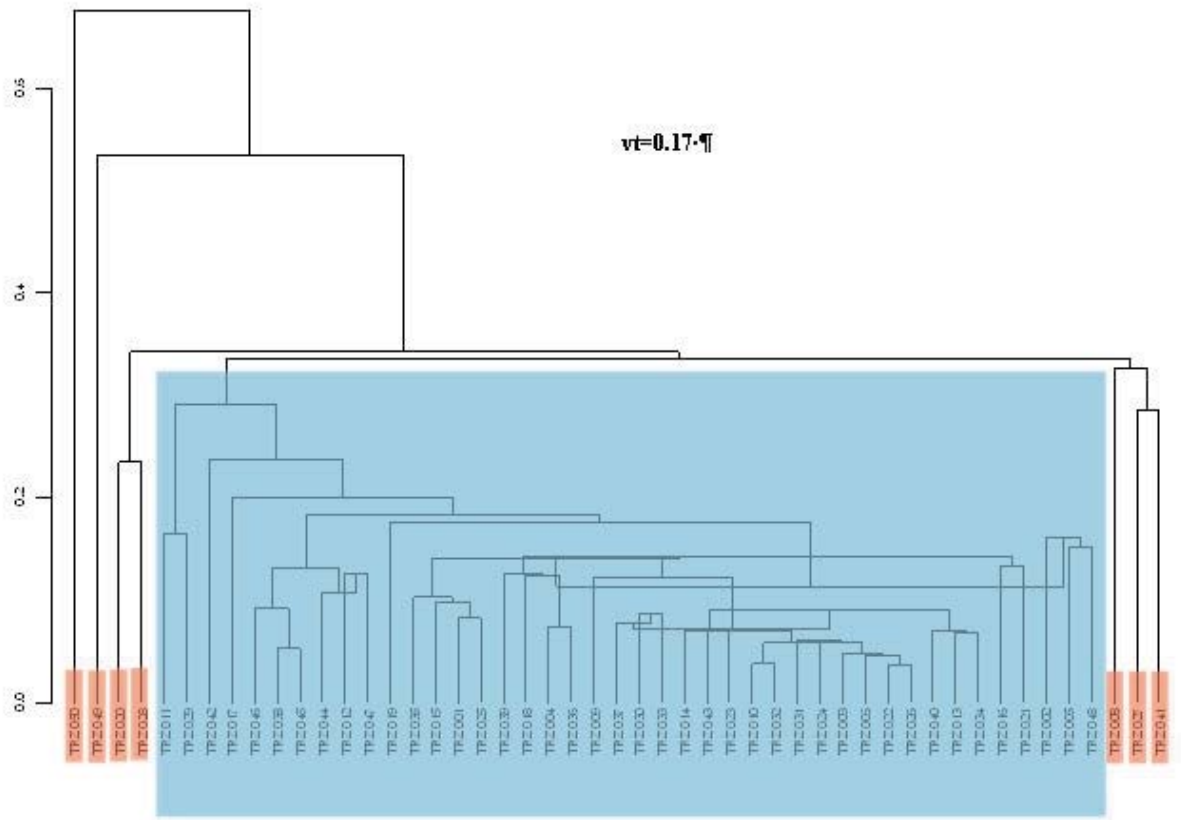

Fig 9: Dendrogram resulting from the cluster analysis performed on the previous subcomposition, using the Squared Euclidean distance and the centroid algorithm, performed by S-plus2000 on the subcomposition: Al_2O_3, MnO, TiO_2, MgO, CaO, Na_2O, K_2O, SiO_2, Ba, Rb, Nb, Zr, Y, Sr, Ce, Ga, V, Zn, Cu, Ni and Cr and Fe2O3, used as a divisor in the logratio transformation.

For the statistical treatment, the chemical data were transformed into logratios following the consideration of Aitchison (1986) and Buxeda (1999) on compositional data, according to the following equation:

$$x \in S^d \rightarrow y = \log\left(\frac{x_{-D}}{x_D}\right) \in R^d$$

where S^d is a d-dimensional simplex (d=D-1) and $\mathbf{x}_{-D}=(x_1,...,x_d)$. The components: Mo, Sn, Co and W were not considered during this transformation owed to possible analytical imprecision and possible contamination during the sample preparation process. Finally P_2O_5 and Pb were not used during the logratio transformation either because of possible postdepositional contamination. Finally, the logratio transformation was performed on the subcomposition: Al_2O_3, MnO, TiO_2, MgO, CaO, Na_2O, K_2O, SiO_2, Ba, Rb, Nb, Zr, Y, Sr, Ce, Ga, V, Zn, Cu, Ni and Cr and Fe_2O_3 was used as divisor, as according to the variation matrix it was the element less contributing to the chemical variability (Buxeda and Kilikoglou 2003). The chemical results are summarized in the dendrogram of Figure 9, resulting from the cluster analysis performed on the previous subcomposition, using the Squared Euclidean distance and the centroid algorithm, performed by S-plus2000 (MathSoft 1999).

Even though the vt of the analysed material is low enough to indicate a one single production or GR (Buxeda, 1995; Tsantini, 2007) as all the ceramic analysed material has been sampled in a specific kiln site, the dendrogram in Figure 9 indicates that there are some individuals (TRZ008, TRZ020, TRZ027 TRZ028, TRZ041, TRZ49, y TRZ50) which are separated from the rest of the material which, in contrary clearly seem to from a one single group (indicated by a blue rectangle in Figure 9). These individuals have been pointed out by red rectangles in Figure 9. Two of them TRZ050 (TZ06KTHP3E1) and TRZ049 (TZ06KTHP12A1), seems to separate in a higher ultrametric distance from the group which indicates significant differences regarding to the group. Nevertheless by looking at the chemical com-

position (Table 2) of these individuals one can observe that their only difference, even though it is important, is a significantly higher concentration in Ba. If we repeat the same cluster analysis, this time, leaving out Ba from the logratio transformation (Figure 10) these two individuals are perfectly integrated into the group. Therefore this single difference in Ba concentration is probably a result of some kind of post-depositional contamination and/or alteration, something we already suspected when we calculated the MCV and saw that the element which was introducing the highest variation in the data set was Ba. That is why both individuals, finally can be classified into the group.

On the other hand, in both Figures 9 and 10 there are two individuals TRZ020 and TRZ028 linked together which seem to be separated in a lower ultrametrical distance from the group. The differences of these two individuals regarding the rest of the ceramics analysed is lower concentrations in K_2O and Rb and higher concentrations in Na_2O. Additionally, it can be observed in the chemical composition (Table 2) that the relationship between the two first (K_2O and Rb) and the last one (Na_2O) is inverse. When both K_2O and Rb are decreasing Na_2O is increasing. This is a chemical indication which could be related to a postdeposictional alteration or/and contamination, normally present in a high fired calcareous pottery. Previous studies (Picon, 1976; Segebade y Lutz, 1980; Lemoin *et al.*, 1981; Scmitt, 1989; Buxeda y Cau, 1997; Buxeda y Gurt, 1998; Buxeda, 1999b; Buxeda *et al.*, 2001; Buxeda *et al.*, 2002; Schwedt *et al.*, 2006) seems to point out that this phenomenon could be the result of leaching of K^{2+} and Rb^{2+} from the amorphous glassy face of the ceramic and the accumulation of Na^{2+} which leads to the formation of a zeolithe called analcyme ($(Na[AlSi_2O_6]\cdot 6H_2O)$) in the pores. However, in the continuation we will confirm this hypothesis by the XRD study. Beside these differences, these two individuals do not present any other difference in their chemical composition regarding the rest of the material. Therefore, we can say that both of them belong to the group.

In order to visualise the chemical differences that the other three non classified individual (TRZ008, TRZ027 and TRZ041) present regarding the main group, finally, in Figure 11, we present the biplot of the first and second principal component. This graph is the result of the principal component analysis applied on the logratio transformed subcomposition: Al_2O_3, MnO, TiO_2, MgO, CaO, Na_2O, K_2O, SiO_2, Rb, Nb, Zr, Y, Sr, Ce, Ga, V, Zn, Cu, Ni and Cr and Fe_2O_3, used as a divisor. TRZ008 is separated by the group because it has a slightly less CaO, Sr, Zn and Cu. TRZ027 because its slightly lower concentration of Ce, Zn, Cu and Cr and, slightly higher concentration in Ga, and, finally, TRZ041 because its differences in the Ce, Zn and Cr concentrations. Nevertheless, the above mentioned chemical differences that each of these individuals present can not be considered significant enough, to not classify all of them into the main group.

As a final conclusion of the chemical study it can be pointed out that, finally all the analysed individuals sampled at the kiln site of *Kara Tepe* are identified into the same homogeneous chemical group which represents the one unique production that represents the Reference Group of this kiln site. The chemical composition and the standard deviations in each element are given in Table 4.

Mineralogical results

The technological aspects of the analysed material have been studied by XRD analysis. From the beginning, it is important to point out that, the analysed ceramic material has a calcareous character (CaO>5-6%). This CaO proportions owed basically to the presence of calcium carbonates facilitate the fromation of calco- and aluminosilicates during the firing process and the formation of a characteristic cellular microstructure proportioning specific physical properties to the material (Maniatis *et al*. 1981; Tite *et al*. 1982).

According to the mineralogical analysis the analysed material can be separate into four basic mineralogical fabrics. The first fabric **F_1** (Figure 12) is characterised basically by the presence of primary minerals (present in the ceramics before firing) and the absence of clear firing phases. Therefore the Equivalent Firing Temperature (EFT) estimated for this group is around the 800/850°C, so it corresponds to a low fired material. The minerals present in this fabric are: calcite, quartz, illite-muscovite, microcline and plagioclase and it contains tree individuals: TRZ050, TRZ039 and TRZ042.

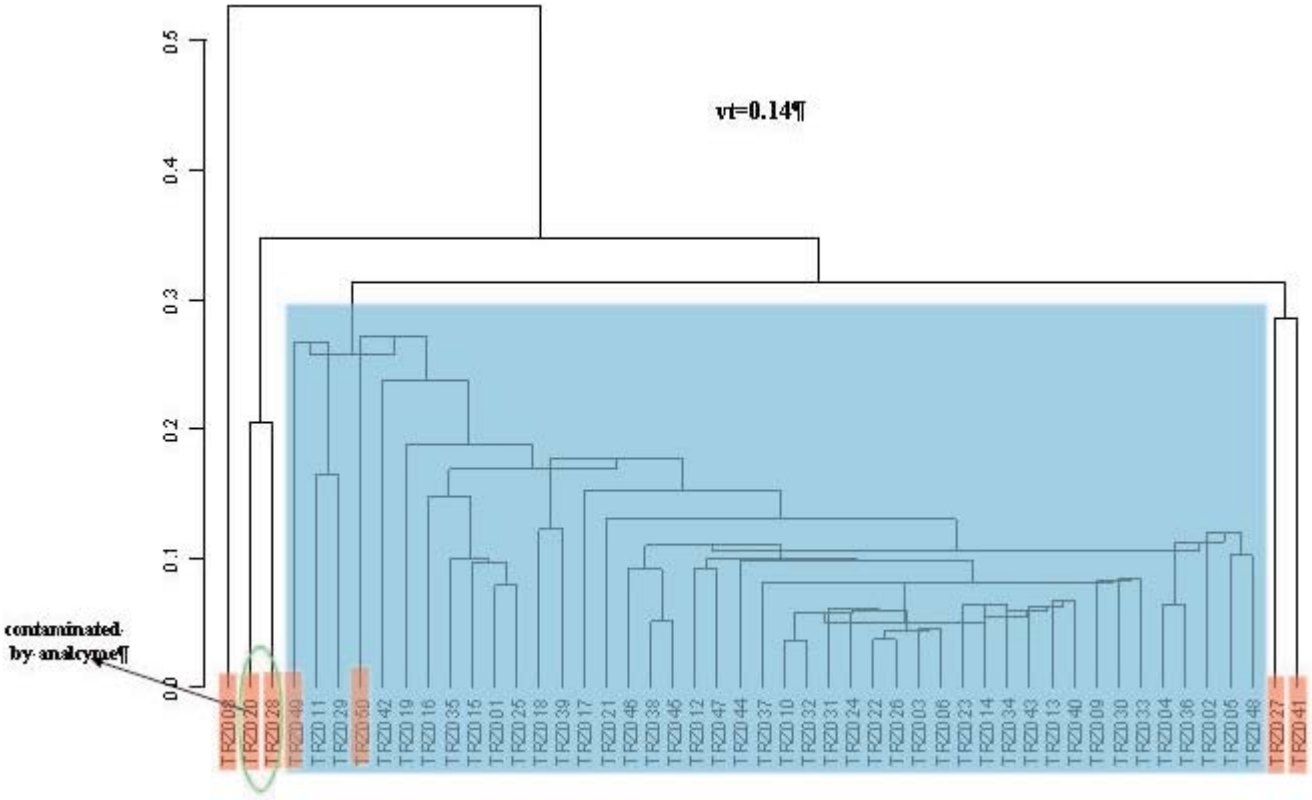

Fig 10: Dendrogram resulting from the cluster analysis performed on the previous subcomposition, using the Squared Euclidean distance and the centroid algorithm, performed by S-plus2000 on the subcomposition: Al_2O_3, MnO, TiO_2, MgO, CaO, Na_2O, K_2O, SiO_2, Rb, Nb, Zr, Y, Sr, Ce, Ga, V, Zn, Cu, Ni and Cr and Fe_2O_3, used as a divisor in the logratio transformation

Elements	Mean	Stan. Desviation
Fe_2O_3%	5,98	0,24
Al_2O_3%	15,62	0,48
MnO%	0,10	0,01
P_2O_5%	0,27	0,07
TiO_2%	0,65	0,02
MgO%	4,05	0,34
CaO%	11,07	1,12
Na_2O%	**1,60** (1,60)*	**0,30** (0,27)*
K_2O%	**3,38** (3,42)*	**0,30**(0,25)*
SiO_2%	57,09	1,28
Ba ppm	**538** (525)*	**99** (72,96)*
Rb ppm	**123** (125)*	**11**(9)*
Th ppm	15	1
Nb ppm	16	1
Pb ppm	19	6
Zr ppm	154	7
Y ppm	29	1
Sr ppm	386	43
Ce ppm	61	9
Ga ppm	22	1
V ppm	103	5
Zn ppm	107	7
Cu ppm	35	4
Ni ppm	50	3
Cr ppm	80	3

* indicates the mean concentrations and the standard deviations without considering the individuals which are contaminated in each element.

Table 4: The mean chemical composition and the standard deviation in each chemical element calculated for the 50 individuals of the Reference Group of kiln site of Kara Tepe.

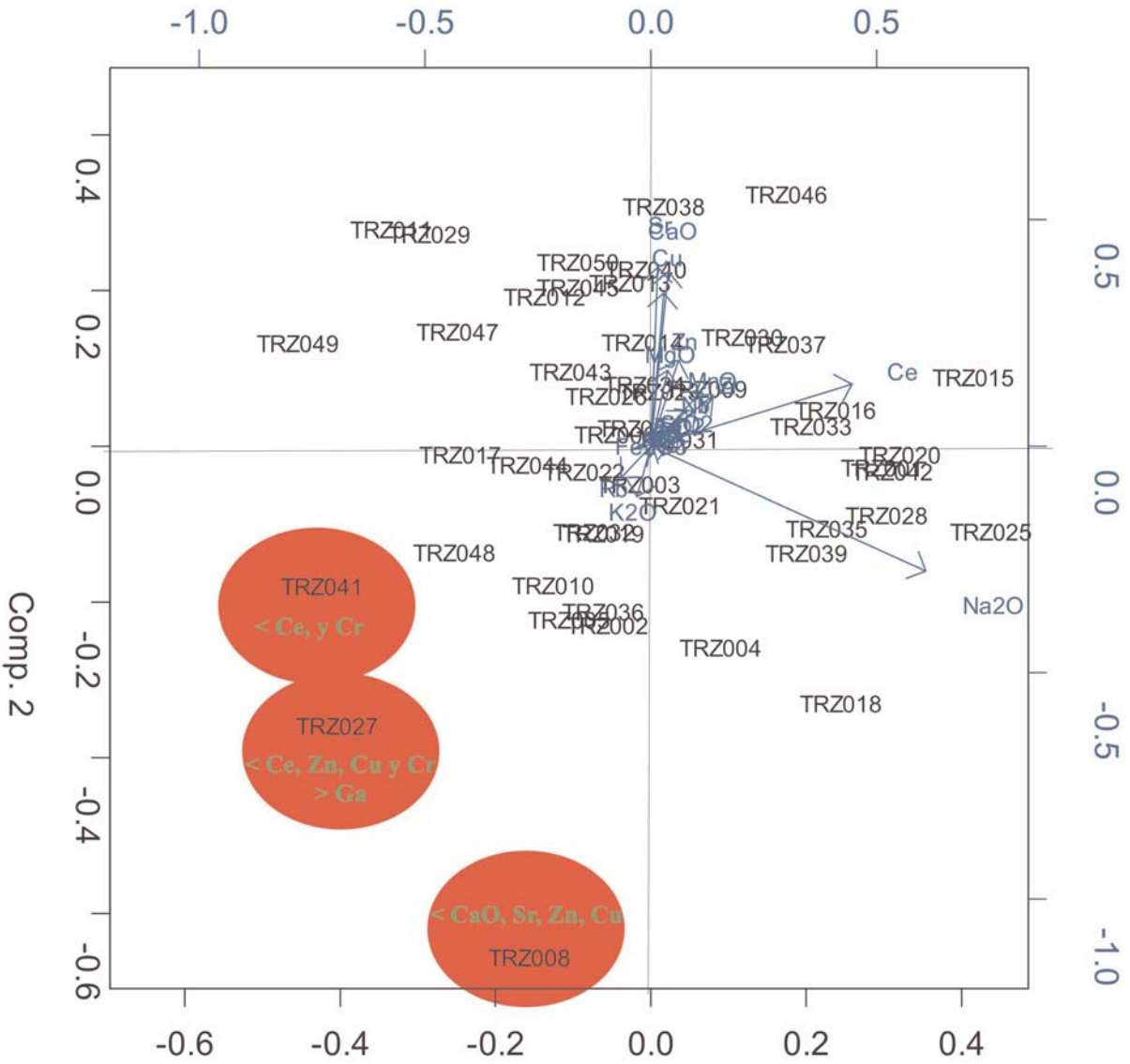

Comp. 1: . Comp. 1 Comp. 1 (VE=0,2749); Comp. 2 (VE=0,2244)

Figure 11: Biplot of the first and second principal component result of the analysis of principal components on the subcomposition: Al_2O_3, MnO, TiO_2, MgO, CaO, Na_2O, K_2O, SiO_2, Rb, Nb, Zr, Y, Sr, Ce, Ga, V, Zn, Cu, Ni and Cr and Fe_2O_3, used as a divisor in the logratio transformation, and without considering the individuals: TRZ050 and TRZ049

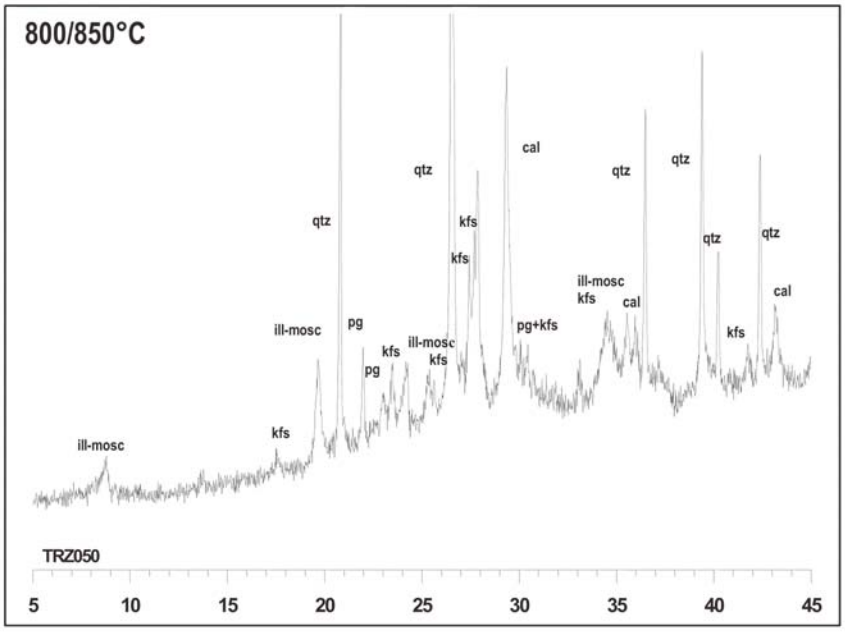

Fig 12: Difractogram of the individual TRZ050, representing F_1

The second mineralogical fabric: **F_2** (Figure 13) is only configured by one individual: TRZ049, in the difrectogram of this individual it can be observed that beside the above mentioned mineral phases there is also a gehlenite in it's indicial phase of formation. Gehlenite is a clear firing phase, that is why the EFT of this fabric is slightly higher that of the previous one. It can be estimated around 850/900°C.

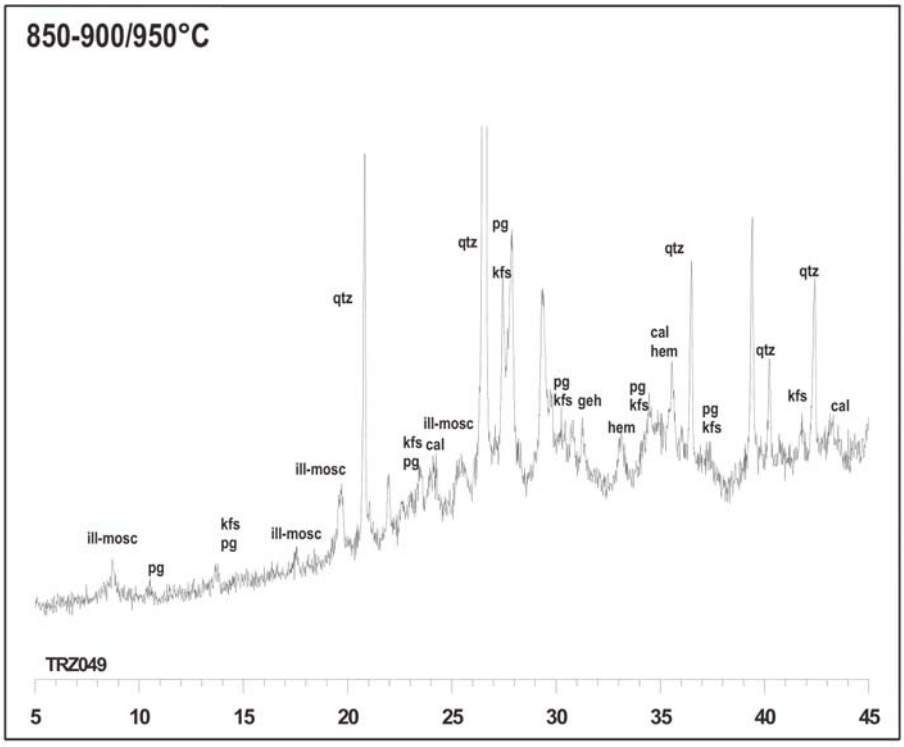

Fig 13: Difractogram of the individual TRZ049, representing F_2

In the third fabric, **F_3** (Figure 14), primary phases, like illite-muscovite and potassium feldspars, and clear firing phases, like gehlenite and pyroxenes appears together in the difractogram of the individuals belong to this fabric (TRZ003, TRZ005, TRZ006, TRZ007, TRZ013, TRZ019, TRZ022, TRZ023, TRZ024, TRZ028 and TRZ031). Therefore, the EFT estimated for this fabric is between 900/950°C and 1000°C.

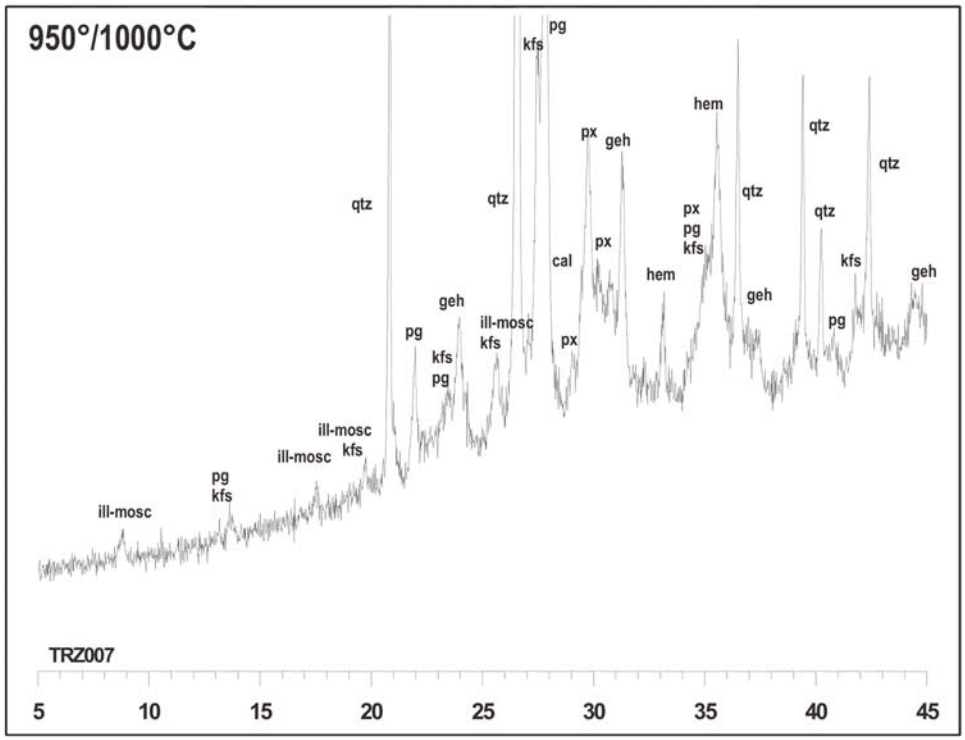

Fig 14: Difractogram of the individual TRZ007, representing F_3

Finally, the last fabric **F_4**, is characterised by the partial decomposition of illite-muscovite, calcite and gehlenite and the clear increment of the pyroxenes as a firing phases of a high temperature (Figure 15). Consequently, this fabric represents over fired ceramics, as the ETF can be estimated over 1000/1050°C and it includes the rest of the individuals. Two of them (TRZ020 and TRZ028) present also analcyme in their difractogram (Figure 15). Analcyme is a zeolith which forms as a result of a postdepositional alteration and/or contamination in the pores of a normally high fired calcareous ceramics. The presence of analcyme justifies the lower concentrations of K_2O and Rb and higher concentrations of Na_2O in these two individuals

It is important to mention that in all the mineralogical fabrics the presence of Hematite is obvious. Hematite is an iron oxide which develops under preferably oxidising atmospheres, that is why, the analysed ceramic material probably manufactured under oxidising then reducing firing atmosphere then again oxidising postfiring conditions. This kind of firing is very normal in a kiln where the fire is in direct contact with the ceramic material. Another observation we have to make is that during firing in this kind of kilns the firing temperature in the laboratory can vary ±150°C depending on the position of the ceramic. Specifically, the temperature is always higher in the central part of the kiln than in the sites. Therefore an ETC estimated in between approximately 850°C and 1000°C, can represent the same firing procedure. That is why, in the case of the Kushan ceramic analysed, sampled at the kiln site of *Kara Tepe*, we can say that even though there are four different mineralogical fabrics indentified according to the mineral phases identified, the process of manufacture of this ceramics is very constant and generally they represent a well/high fired ceramic material.

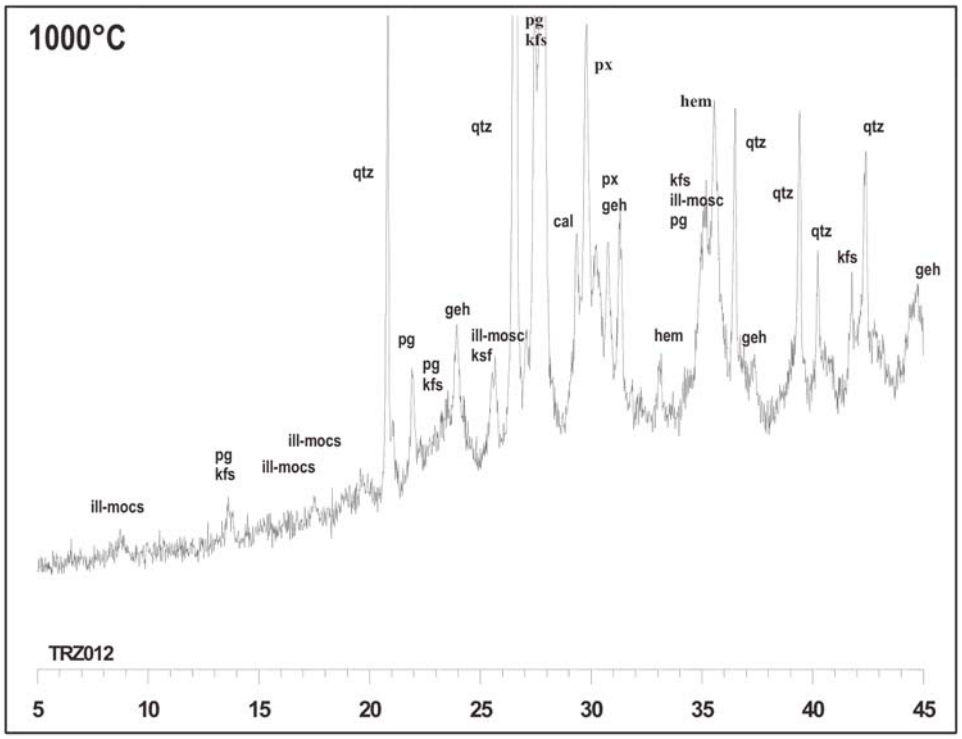

Fig 15: Difractogram of the individual TRZ012, representing F_4

Results of the study by Scanning Electron Microscopy and EDAX

Firing process (firing temperature and atmosphere) brinks important changes to the microstructure of the ceramic matrix (Maniatis *et al.*, 1981; Tite *et al.*, 1982). With the increment of the temperature the sinterisation process starts (the clay particles start to "fuse" together). This progressively leads to the vitrification of the matrix. On the other hand, the microstructure which develops in calcareous ceramics (made with calcareous clay) is different than in the border or non calcareous ones. Generally in calcareous ceramics excess in CO_2 produced by the decomposition of the carbonates normally leads to the development of a cellular type microstructure, opposite to the non calcareous pottery where the vitrified phase is normally compact and continuous. The microstructure affects significantly the physical and mechanical properties of the fired product, thus the adequacy of a pottery to a concrete function among other aspects depends directly on its microstructure.

The results of SEM are given according to the observations of the fresh fractures of one characteristic individual selected for each mineralogical fabric, estimated by XRD. Microphotographs of a Secondary Electron (SE) image at 2000x magnification are presented in each case.

TRZ050 (TZ06KTHP3E1) is the individual representing the first mineralogical fabric studied by SEM-EDAX. According to XRD this is the lowest fired individual in the whole set of the analyzed individuals. The microphotograph (x2000) of the Figure 16 shows a non vitrified microstructure which indicates a firing temperature that does not exceed the 750/800°C. The chemical microanalysis by EDAX in concrete surface areas also revealed the presence of NaCl crystals. The presence of NaCl was confirmed in the most of the samples analyzed by SEM-EDAX, as we will se following. The high Na concentration in the whole set of the analyzed material can be confirmed by observing the raw chemical data (Table 2).This high concentration of Na though, only can be related to the presence of analcime as a secondary mineral formed during postdeposition in two cases (TRZ020 and TRZ028). Therefore, the generally high concentrations in Na in the rest of the individuals might be explained by the presence of these NaCl crystals. The presence of these crystals most likely can be the result of postdepositional alteration and/or contamination due to the high concentrations of NaCl in the specific geographical area where the ceramics were discovered. In the deserts the high salt concentrations are ordinary and that can be the reason for this specific alteration and/or contamination process. Additionally, the formation of a zeolithe called analcyme ($Na_2AlSi_2O_6 \times H_2O$) in the higher fired ceramics, therefore,can be a consequence of this NaCl presence, which leaded to the leaching of K^{2+} and Rb^{2+} from the amorphous glassy face of the ceramic and the accumulation of Na^{2+}.

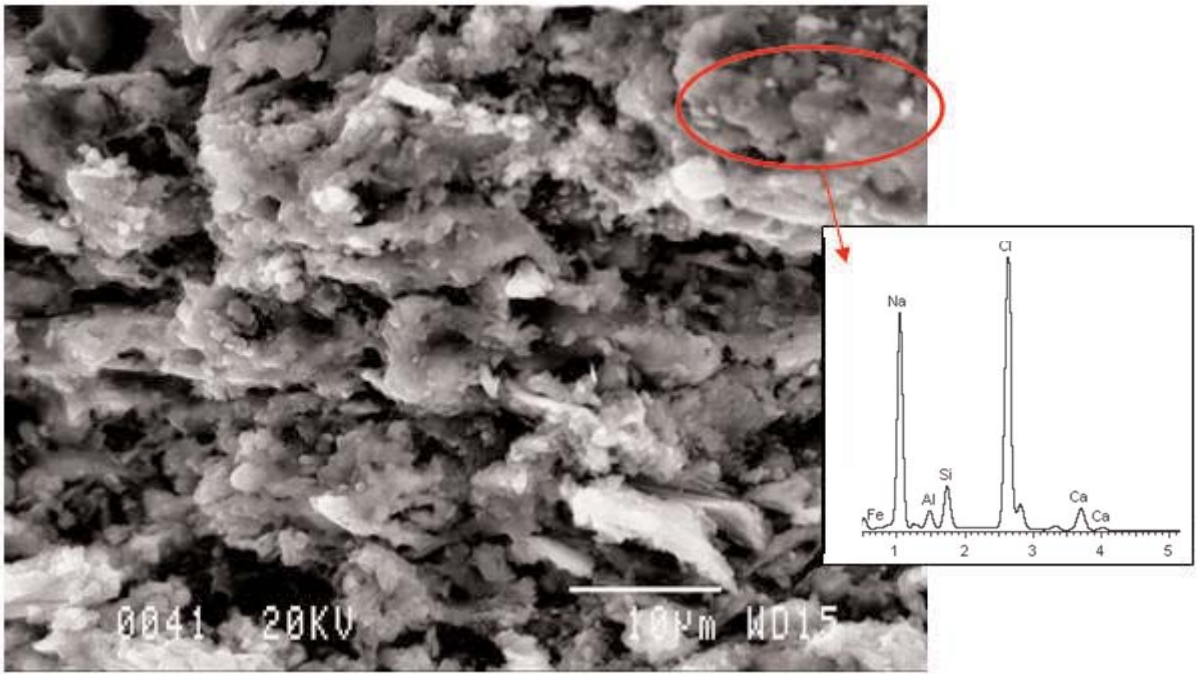

Fig 16: Microphotograph (x2000) of the SE image of the matrix of the individual TRZ050

TRZ049 is the only individual that configures the second mineralogical fabric. Its microstructure can be observed in the microphotograph of Figure 17. This individual unlike the fist one, already clearly exposes vitrification, therefore the firing temperature in this case is obviously higher that in the case of the first individual (≥900°C).

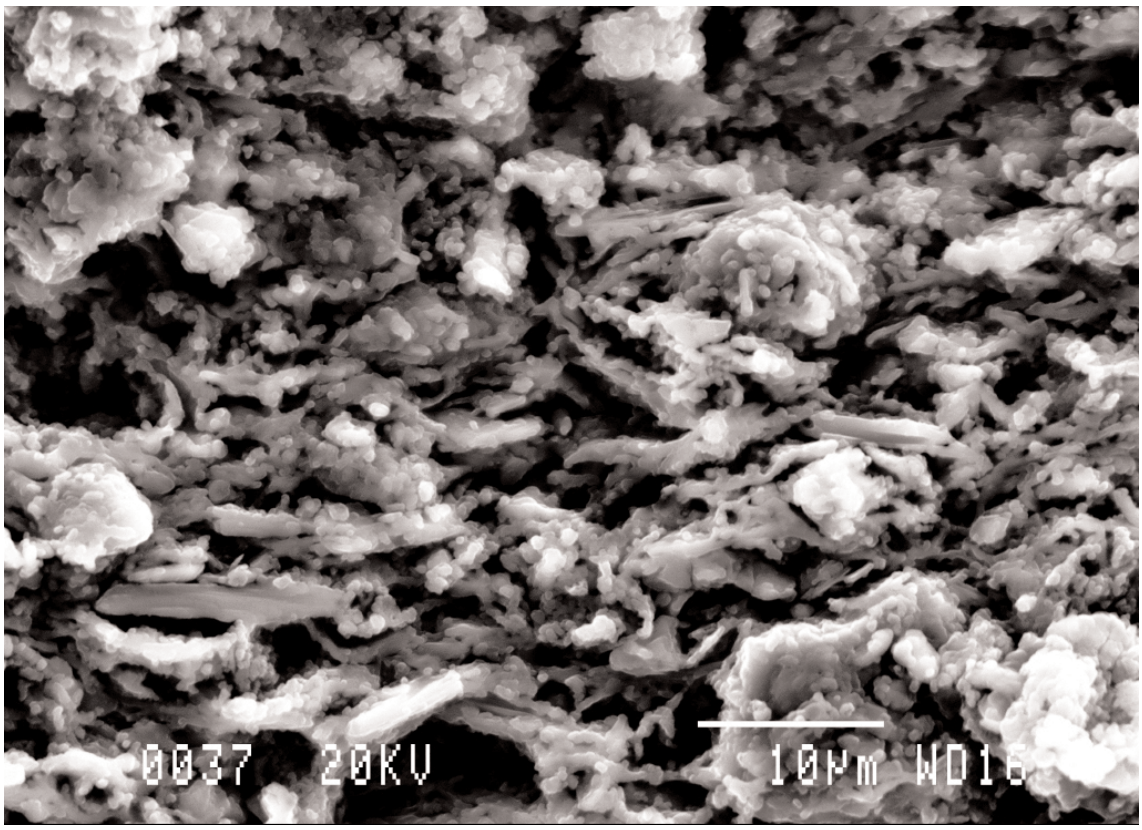

Fig 17: Microphotograph (x2000) of the SE image of the matrix of the individual TRZ049

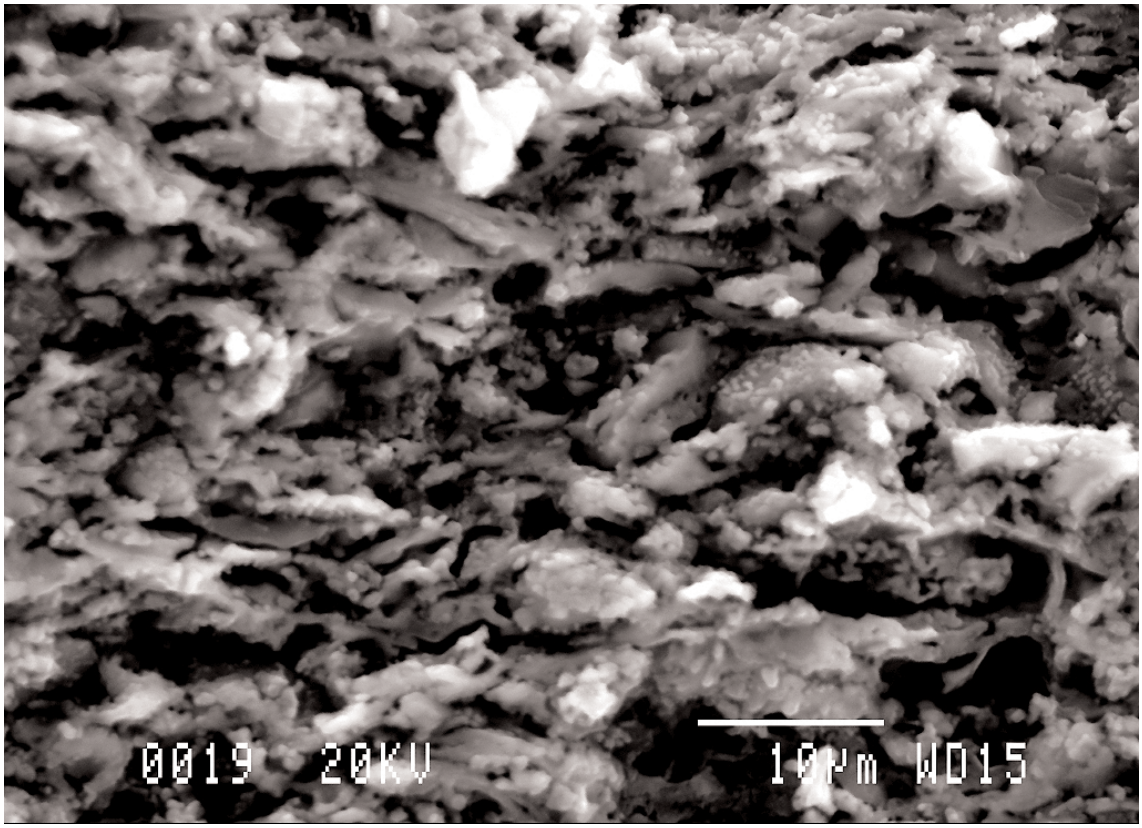

Fig 18: Microphotograph (x2000) of the SE image of the matrix of the individual TRZ022

The next mineralogical fabric **F_3** is represented by the individual **TRZ022**. In the microphotograph (Figure 18, centre) of the matrix of this individual one can observe the presence of slightly more extended glassy phase which indicates a little bit higher firing temperature (≥950°C). By looking at the microphotograph of the individual **TRZ020** under lower magnification (x1000) (Figure 11) of a sample has been taken from this individual, very bright particles regarding to the ceramic matrix can be distinguished, all over the fresh fracture's surface. These bright particles that are given by the SE image, under a higher magnification (x2000), have rather rectangular shape or asymmetrical shape (site figures in Figure 19). The chemical microanalysis preformed by EDAX in all these crystals have given high concentrations of Na and Cl, exactly the same way that in the case of **TRZ050**, therefore most likely they correspond to well crystallised NaCl (salt) indicating once again post depositional contamination and alteration.

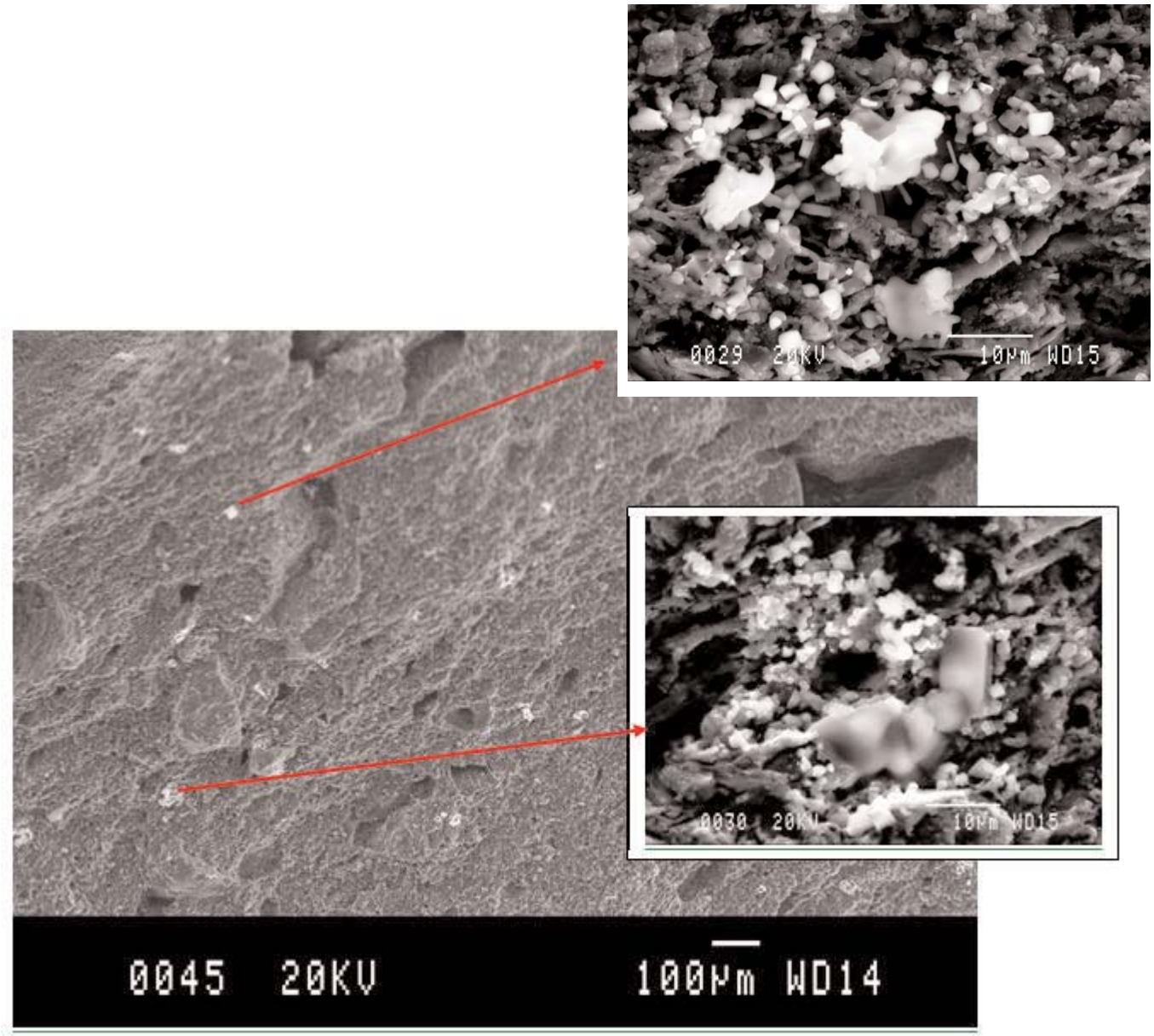

Fig 19: Microphotograph (x1000) of the SE image of the matrix of the individual TRZ022, and microphotographs (x2000) of the NaCl crystals

Finally the last individual studied by SEM is **TRZ028**, which is representing one of the altered and or contaminated with analcime individual belonging to the mineralogical fabric $\mathbf{F_4}$ that contains all the over-fired ceramic individuals. At first site (Figure 20) the microstructure of this individual exposes extended vitrification but it is also indicates some kind of alteration as it is covered by this spherical particles (Figure 21), that after the microanalysis with EDAX seem to have a very high concentration in Ca and they might be secondary calcite. The extended vitrification indicates that this individual is high fired (≥1000/1050).

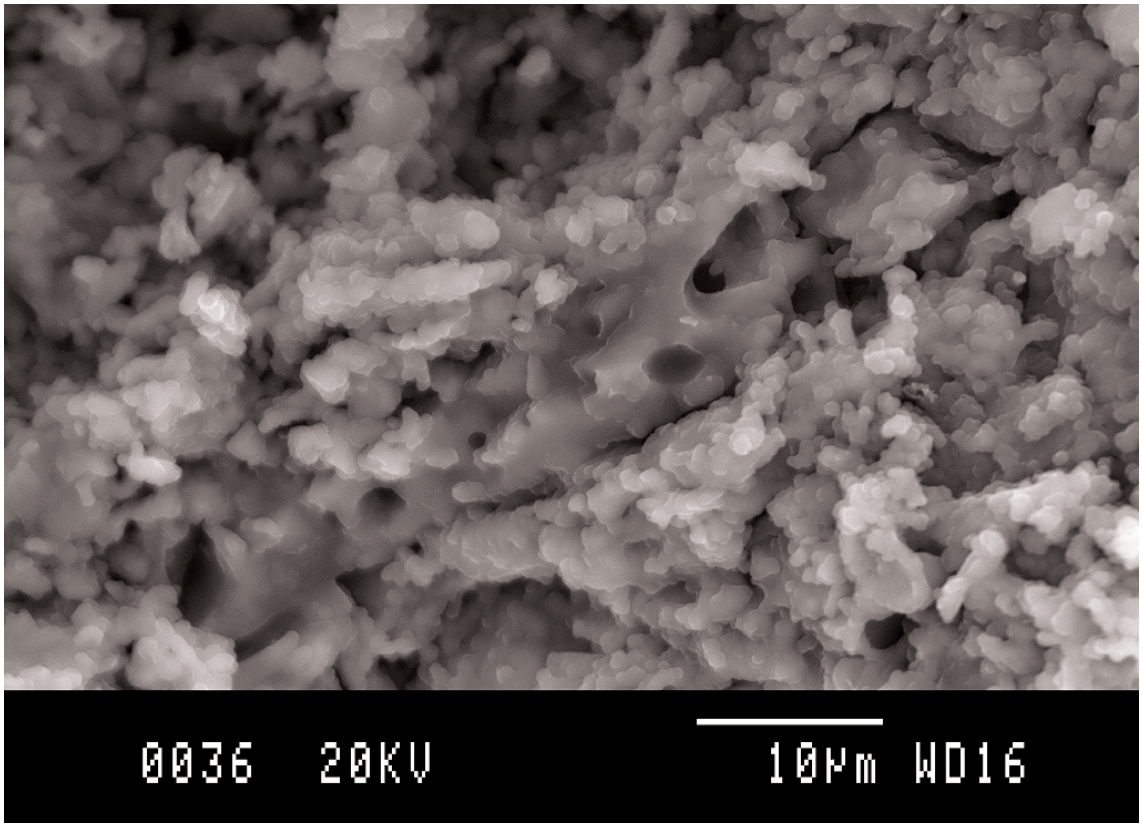

Fig 20: Microphotograph (x2000) of the SE image of the matrix of the individual TRZ028

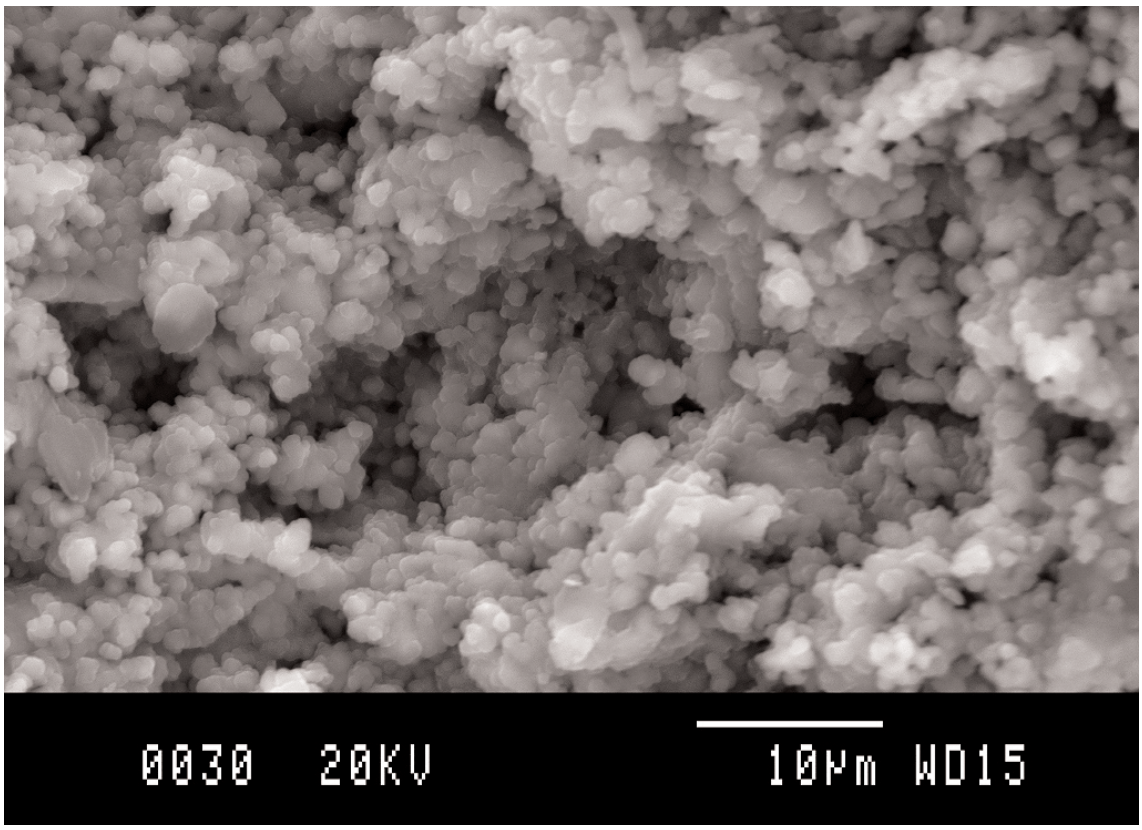

Fig 21: : Microphotograph (x2000) of the SE image of secondary calcite in the matrix of the individual TRZ028

By XRD we have been able to identify the presence of analcyme in this individual. However, analcyme is cryptocrystalline, thus we can not identify it by SEM. On the other hand it is important to mention that from all the individual studied by SEM this is the only one without the presence of NaCl crystals in its matrix, therefore it is possible to assume that the formation of this zeolithe ($Na[AlSi_2O_6]\cdot 6H_2O$) can be a consequence of the decomposition of the accumulated NaCl and its transformation to analcyme by the interaction with the amorphous glassy face.

Conclusions and Discussion

The final conclusion after the chemical study is that all the individuals analysed in this work are classified in the same production, which is identified as the Reference Group (RG) of the kiln of *Kara Tepe*, as all the material analysed were sampled at this production centre. The composition of this RG is given in Table 4. During the chemical study we could identify two different alteration and/or contamination processes, which have been affected specific individuals. The first process is related to the increment of Ba in the ceramic composition and the second is related to the decrease of K_2O and Rb and the increment of Na_2O. The last alteration and/or contamination process is related to growth of crystals of a specific zeloithe called analcyme.

The conclusions which can be done after the mineralogical study on the aspects of manufacture of these ceramics is that they generally represent well to high fired ceramic material, fired between 850°C and 1050°C. The firing conditions are preferably oxidising. There are only three individuals fired at a low temperature. However, according to the mineralogical composition, we could distinguish between four different mineralogical fabrics, each related to a specific range of Equivalent Firing Temperature.

The generally high fired and calcareous character of the analysed material could be confirmed by the study with SEM. The presence of NaCl crystals as a result of a possible postdepositional contamination and/or alteration in most of the individuals studied by this technique could be also confirmed. In fact, the only individual studied by SEM which did not present NaCl crystals in its matrix was the one which had analcyme in its mineralogical composition according to XRD (TRZ028). Therefore it is possible to assume that the formation of this zeolithe can be a consequence of decomposition of the accumulated NaCl and its transformation to analcyme by the interaction with the amorphous glassy face.

The achaeometrical characterisation, finally, for the first time, has permitted the establishment of the Reference Group of the production of the kiln site in *Kara Tepe*, which is the first *Kushan* ceramic well identified ceramic production at the whole area. This leads to the existence of a clear local pottery production at the site. On the other hand, this work illustrates also the main aspects of the pottery production at the area and permits to design further studies on the definition of consumption and distribution patterns first in a local level, then in a broader area. For that, it is important to broaden this study, in the future, including the archaeometrical study of ceramics coming from the archaeological site of Termez and then, to study other proximate and farther located production sites.

References

Abdurazakov, A. A., 1987, "Khimicheskie sostavy keramiki i glazurej arkhitekturnykh pamjatnikov Uzbekistana", *IMKU* 21.

Abdurazakov, A. A., 1988, "Khimicheskie sostavy rannesrednevekovykh stekol Srednej Azii", *IMKU* 22, pp. 205-211.

Abdurazakov, A. A., 1996, "Khimicheskie sostavy srednevekovykh stekol Kara-tepe (X-nachalo XIII v.)" in : *Kara-tepe* VI, pp. 301-306.

Abdurazakov, A. A., Bezborodov, M. A., Zadneprovskij, Ju. A., 1963, *Steklodelie Srednej Azii v drevnosti i srednevekov'e*, Tashkent, IAN UzSSR.

Abdourazakov, A., 2001, "La production artisanale en Bactriane-Tokharestan. Résultat des études chimiques et des restaurations", in : *La Bactriane au carrefour des routes et des civilisations de l'Asie centrale*, pp. 399-403

Abdurazakov, A. A., Dzhalalova, S., 1986, "Issledovanie khimicheskikh sostavov drevnej bytovoj keramiki juga Uzbekistana", *IMKU* 20, pp. 205-210.

Aitchison, J., 1986, *The Statistical Analysis of Compositional Data*, Chapman and Hall, London.

Aitchison, J., 1992, On Criteria for Measures of Compositional Difference, *Mathematical Geology*, 24, 365-379.

Ariño E., Sala R., Lafuente M., Gurt J.-M., Pidaev Sh., Stride S., 2007, The Ceramic Kilns of Kara Tepe, in IPAEB, Volume I: *Preliminary Report of the First Season work of the International Pluridisciplinary Archaeological Expedition to Bactria*, J.M. Gurt I Esparaguerra, S. Pidaev and S. Stride (eds), Barcelona.

Buxeda i Garrigós, J., 1995, *La caracterització arqueomètrica de la ceràmica de Terra Sigillata Hispanica Avançada de la ciutat romana de Clunia i la seva contrastació amb la Terra Sigillata Hispanica d'un centre productor contemporani, el taller d'Abella*, Col·lecció de Tesis Doctorals Microfitxades, 2524, Universitat de Barcelona, Barcelona.

Buxeda i Garrigós, J. (1999b) Problemas en torno a la variación composicional, en J. Capel Martínez (ed.), *Arqueometría y arqueología*, p. 305-322, Monográfica de Arte y Arqueología, 47, Universidad de Granada. Granada.

Buxeda i Garrigós, J. y Cau Ontiveros, M. A. (1997). Caracterización arqueométrica de las ánforas T-8.1.3.1del taller púnico FE-31 (Eivissa), en J. Ramon Torres, FE-13: *un taller alfarero de época púnica en Ses Figueretes (Eivissa)*, p. 173-192, Treballs del Museu Arqueològic d'Eivissa i Formentera 39, Govern Balear, Conselleria d'Educació, Cultura i Esports.

Buxeda i Garrigós J., y Gurt Esparraguera, J., M., La caracterització arqueomètrica de les àmfores de Can Peixau (Badalona) i la seva aportació al coneixement de la producció Pascual 1 al territori de Baetulo, en M. Comas y P., Padrós (coord.), *El Vi a l'Antiguitat, Economia, Producció i Comerç al Mediterrani Occidental* (II Col·loqui d'Arqueologia Romana), p. 193-217, Monografies Badalonines, 14, Museu de Badalona, Badalona.

Buxeda i Garrigós J., Kilikoglou V. y Day P., M. (2001). Chemical and mineralogical alteration of ceramics from Late Bronze age kiln at Kommos, Crete: the effect on the formation of a Reference Group, *Archaeometry*, 43, 349-371.

Buxeda i Garrigós, J. i Kilikoglou, V., 2003, Total Variation as a Measure of Variability in Chemical Data Sets, a L. van Zelts (ed.), *Patterns and Process: a Festschrift in honour of Dr. Edward V. Sayre*, Smithsonian Center for Materials Research and Education, Suitland, Maryland, pp.185-198.

Hein, A., Tsolakidou, A., Iliopoulos, I., Momsen, H., Buxeda, J., Montana, G., Kilikoglou, V., **2002,** Standardisation of elemental analytical techniques applied to provenance studies of the archaeological ceramics: an inter laboratory calibration study, Analyst, 127, 542-553.

LEMOINE C., MAILLE, E., POUPET P., BARRANDON, J. N. Y BORDERIE, B. (1981). Étude de quelques altérations de composition chimique des cerámiques en milieu marin et terrestre, *Revue d'Archéométrie*, Suppl. S, 349-360.

PICON, M., 1973, *Introduction à l'étude tèchnique des céramiques sigillées de Lezoux*, Centre de Récherches sur les Téchniques Greco-Romaines, 2ª edició, Université de Dijon, Dijon.

PICON, M., 1984, Problèmes de détermination de l'origine des céramiques, in T. Hackens, M. Schvoerer (Eds.), *Datation-caractérisation des céramiques anciennes Cours Intensif Européen* (Bordeaux, Talence 1981), PACT Nº 10, Paris, pp. 425-433

SEGEBADE, C. Y LUTZ, G. J. (1980). Photon activation analysis of ancient Roman pottery, en E. A. Slater and J. O. Tate (eds.), *Proceedings of the 16th International Symposium on Archaeometry and Archaeological Prospection* (Edinburg, 1976), National Museum of Antiquities of Scotland, p. 20-29.

SCHMITT, A. (1989). *Méthodes géochimiques, pétrographiques, et mineralogiques appliquées à la détermination de l'origine des céramiques archéologiques*. Thèse de Doctorat, Université de Bordeaux III, Bordeaux.

SCHWEDT, A., MOMMSEN, H., ZACHARIAS, N., BUXEDA, J., 2006, Analcime crystallization and compositional profiles-comparing approaches to detect post-depositional alterations in archaeological pottery, *Archaeometry*, 48, 2, 237-251.

TSANTINI, E., 2007, *Estudi de la producció i la distribució d'àmfores ibèriques en el NEpeninsular a través de la seva caracterització arqueométrica*, Tesis Doctoral, Josep Maria Gurt i Esparraguera i Jaume Buxeda i Garrigós (Directors), Universitat de Barcelona, Barcelona.

VIVDENKO, S. V., 1987, "Primenenie spektral'nogo analiza dlja izuchenija keramiki Severnoj Baktrii", in: *Gorodskaja kul'tura Baktrii-Tokharistana i Sogda*, pp. 38-41

VIVDENKO, S. V., 1987, "Elementarnyj sostav severobaktrijskoj keramiki", in : *A. S Sagdullaev, Usad'by Drevnej Baktrii*, Tashkent, Fan, pp. 96-98.

VIVDENKO, S. V., 1990, *Issledovanie i restavratsija kushanskoj plastiki severnoj Baktrii*, AKD, Tashkent.

VIVDENKO, S. V., 1992, "*I*ssledovanie drevnikh tekhnologij Severnoj Baktrii", in: *Srednjaja Azija i mirovaja tsivilizatsija*, pp. 36-37.

VIVDENKO, S. V., 1993, "Opredelenie temperatury obzhiga Severo-baktrijskoj keramiki", in : *Vestnik Shelkovogo Puti*, pp. 124-126.

VIVDENKO, S. V., 1994, "A technological Examination of the Plastic Art of North Bactria in the Kushan Period", *SRAA* 3 (1993/1994), pp. 143-155.

VIVDENKO, S. V., 1996, "La technologie de la création de la sculpture en argile", in : *La Bactriane de l'hellenisme au bouddhisme*, pp. 42-47.

Datation by C14 of samples comming from the archaeological context of the Kiln Nº2 of Kara Tepe

Joan S. Mestres, Anna M. Rauret

This report describes the dating by the Laboratory of Radiocarbon Dating of the University of Barcelona of five samples of charcoal from the site of Termez (Uzbekistan), handed in by Dr. Anna Maria Rauret Dalmau. The identification of the materials and the amount received of each one is indicated, respectively, in the first and the second columns of Table I.

1. Context of the Material and Aim of the Dating

The material in question comes from various strata of a kiln situated in a ceramics workshop and the aim of the analysis is to establish its absolute chronology.

2. Description and Treatment of the Material

The material received was formed by fragments of charcoal of varying size none of which was superior to 41 mm in its maximum dimension. The fragments of charcoal were mixed with loose or compact earth or gravel, apart from the last sample where they were contained in a matrix of ash.

TABLE I
Treatment of the materials

Identification of Material	Original Material	Separated Charcoal, totally or partially (g)	Net Charcoal (g)	Purified Charcoal (g)	Yield in purified charcoal (g)
UE 9	230,4	50,215*	49,414	39,618	80,18
UE 9	14,5	13,252	13,001	9,003	69,23
UE 11	19,1	16,083	15,998	9,8	62,4
UE 12	2 ,5	2,1			
UE 14	99,2	3,248	3,218	1,442	44,81

*Charcoal partially separated

The materials which are analysed are submitted to a treatment with two main aims. The first one is to eliminate contamination caused by foreign components produced by chemical compounds of indeterminate age coming from the exterior environment as well as to eliminate contamination due to possible manipulations of the material after its extraction. The second one is to isolate with maximum integrity the most representative constituent of the material to be dated.

So as to separate the charcoal from its gangue, the larger fragments of charcoal were extracted from the first sample until the amount indicated in the third column of Table I was obtained. The earthy fragments were separated from the second sample using pincers until the charcoal was free. The adherent earth on the surface of the fragments of charcoal of the third sample was removed using a soft brush. The fragments of charcoal of the fourth sample were separated from the grains of sand by passing them through a 0,25 mm sieve. The fifth sample was passed through 2, 1 and 0,5 mm sieves. The fragments

of charcoal larger than 0.5 mm were extracted systematically with pincers whereas only the larger ones of the rest were extracted. The total amount of charcoal extracted from each sample is indicated in the third column of Table I. As far as possible, the surface of the larger fragments of charcoal was brushed with a soft brush so as to eliminate dust. In order to enable the observation and elimination of possible intrusions of foreign elements the larger fragments of charcoal were broken along their natural breaking surfaces. The fourth sample, due to its reduced amount and the low yield expected of purified charcoal - see sample UE 14, sixth column- was abandoned. Finally the clean material, the weight of which is indicated in the fourth column of Table I, was grinded down to dust.

The pulverised material was then treated with 2M hydrochloric acid at 95ºC during 24 hours so as to eliminate the carbonates coming from water circulation and/or soil and the soluble in acid material fraction. So as to eliminate possible humic acids coming from the vegetative cover of the earth, the insoluble residue of the acid treatment was suspended in water and was treated with successive additions of 2M or 1M ammonia at room temperature until the pH of the solution was high enough to guarantee the total elimination of all acid substances. Finally the resulting product of this treatment was boiled with 0,4M hydrochloric acid in order to eliminate the carbonates of atmospheric origin. Thus a residue of purified charcoal, exempt of carbonates and humic acids and ready for dating, was obtained, whose weight is indicated in the fifth column of Table I,.

3. Preparation of the measurement of the radioactivity. Synthesis of benzene

As it is not possible to measure the radiocarbon contents directly from the purified charcoal, this is transformed into an adequate chemical compound which enables the measurement of the activity due to the ^{14}C through of liquid scintillation. We will now describe the chemical process which leads to the preparation of this chemical compound: benzene

The adequate amount of purified charcoal was burned in combustion system under oxygen pressure. The resulting carbon dioxide, purified and dried, was left three weeks in order to take place the radioactive decay of the ^{222}Rn which may have been present. After this, the isotopic abundance of ^{13}C of the material was measured by mass spectrometry in a small sample of carbon dioxide. Later the remaining carbon dioxide was reduced with metallic lithium to lithium carbide, this was hydrolysed to acetylene with water of low tritium content and finally the acetylene was catalytically trimerized to benzene (MESTRES *et al.,* 1991).

4. Radiometric measurements

In order to measure the radioactivity of the benzene produced by the synthesis described above and which contains the carbon present in the material being dated, this, if the quantity obtained is lower than 5,2 ml, is diluted gravimetrically with inactive benzene analytical reagent up to 5,2 ml. With this mixture or directly with the benzene obtained during the synthesis, the the activity measurement solutions were prepared weighing 5.000 ml which are added to low potassium content glass vials together with the adequate amounts of the scintillators Bu-PBD and Bis-MSB in solid form, previously weighed.

Oxalic Acid II, supplied by the National Institute of Standards and Technology (USA) was used as a reference substance for the measurement of initial activity. It is oxidized into carbon dioxide with a solution of potassium permanganate and later transformed into benzene in identical manner to the samples (loc. cit.). The preparation of the solution for the measurement of initial activity is also undertaken in identical manner to the samples.

The value of the background associated to each vial is determined through the measurement of two reference blank solutions prepared in identical manner to the samples, but using inactive benzene for the solution of the measurement.

The samples, two standards of initial activity and the two reference blanks for the measurement of the background are counted during a period of 50 hours each, divided into intervals of 50 minutes in a LKB-Wallac 1217 Rackbeta liquid scintillation counter. The efficiency of the measurement is determined during each interval by an efficiency calibration curve in function of the quenching previously established with activity standards prepared in the same laboratory (loc. cit.)

5. Results and Discussion

The results of the measurement of the isotopic abundance of ^{13}C ($\delta^{13}C$) and the results of the counting and measurement of the radioactivity, along with its incertitude expressed as a once the standard deviation (loc. cit.), are given in Table II. It can be observed that the value of the isotopic abundance of ^{13}C measured in the sample is normal for charcoal, for which it is situated between -23 and 27‰ (STUIVER I POLACH, 1977).

Table II
Result of radiometric measures

Sample	$\delta^{13}C$ (‰)	Amount of benzene measured (g)	C count (cpm)	Background (cpm)	Net count Rate (cpm)	Efficiency of count (%)	Normalised rate of count of benzene, **AsN** (cpm/g)	Normalised rate of count of benzene, **A0N** (%)
UE 9	-25,131	4,3919	30,599±0,106	2,873±0,044	27,73±0,12	72,857±0,030	8,667±0,036	10,612±0,031
UE 9	-25,966	4,3980	30,038±0,092	2,921±0,042	27,117±0,101	72,863±0,029	8,478±0,032	10,595±0,027
UE 11	-25,640	4,3978	30,680±0,094	2,915±0,042	27,765±0,102	72,854±0,034	8,677±0,032	10,595±0,027
UE 14	-25,061	0,54045	6,184±0,36	2,876±0,041	3,308±0,055	72,879±0,018	8,40 ±0,14	10,595±0,027

The calculation of the radiocarbon date is based on the experimental results given in Table II and responds to the following equation:

$$R = \frac{T_{1/2}}{\ln 2} \times \ln \frac{A_{0N}}{A_{SN}} \qquad \textbf{(T½ = 5568 anys)}$$

Where A0N represents the initial activity and ASN represents the residual activity in the dated material, corrected by isotopic fractionation of the ^{14}C.

The application of the previous equation to the measurement results enables to calculate the radiocarbon date. The results of the dating and the code of the dates, assigned by the laboratory are given here:

Termez –

UE 9	**UBAR-916**	**1625 ± 40 BP**
UE 9	**UBAR-929**	**1790 ± 35 BP**
UE 11	**UBAR-930**	**1605 ± 35 BP**
UE 14	**UBAR-931**	**1870 ± 130 BP**

The results given here only concern the received samples.

6. Calibration of the Radiocarbon Date and Evaluation of the Result

Dating by radiocarbon is based on a fundamental hypothesis, which is the supposition that that specific content of radiocarbon present in the materials which can be dated has remained constant over time. Since this hypothesis is not entirely exact, but there have been fluctuations of this content over time, the dates calculated on the basis of this hypothesis have a conventional character since they deviate from the dates expressed in the solar chronological scale and define the so called radiocarbon chronological scale. By measuring the radiocarbon age of tree-rings of known age thanks to dendrochronology, it has been possible to establish a curve, which currently covers the past 12400 years (Reimer et al., 2004) and which relates the conventional radiocarbon dates with the dates expressed according to the solar chronological scale. This curve, called calibration curve, is not monotonous and does not establish a univocal relationship between both chronological scales, but it enables to each radiocarbon date to be associated with more of one solar date.

Because of its non lineal character and the lack of monotony of the calibration curve, the probability distribution of the true calibrated radiocarbon around the single or several experimental calibrated dates is not a Gaussian distribution, as in the case of the probability distribution of the true radiocarbon date. The probability distribution of the true calibrated date is an asymmetrical complex distribution, which can present different modes, around which one or several intervals of probability are defined. The width of these intervals are defined in such a way that the sum of the probabilities that the true calibrated that falls in any of them be 68,3% or 95,4% (Stuiver and Reimer 1993); these values are chosen by analogy with the probability distribution of the radiocarbon date and correspond to the probability that the true radiocarbon date falls in an interval of time, which centred on the experimental radiocarbon date has an amplitude equivalent respectively to two or four times the standard deviation.

Table III shows the results of the calibration of the radiocarbon dates.

- Column A and B: Reference of the sample and code of the radiocarbon date assigned by the laboratory.
- Column C: Radiocarbon date with its uncertainty expressed as standard deviation
- Column D: Experimental calibrated date, corresponding to the intersection of the experimental radiocarbon date with the calibration curve. It corresponds to the maximum modes on the probability distribution of the calibrated date.
- Column E and F: Intervals of the Calibrated Date centred on the probability distribution mode of the true calibrated date corresponding to a total probability of 68,3% and probability associated to each interval, respectively.
- Column G and H: Intervals of the Calibrated Date centred on the probability distribution mode of the true calibrated date corresponding to a total probability of 95,4% and probability associated to each interval, respectively.

Table III
Calibration of Radiocarbon Dates

A	B	C	D	E	F	G	H
UE 9	UBAR-916	1625± 40 BP	cal AD 420	cal AD 386–442 cal AD 452–461 cal AD 484–532	37,9% 3,7% 26,7%	cal AD 268–271 cal AD 335–542	0,2% 95,2%
UE 9	UBAR-929	1790± 35 BP	cal AD 238	cal AD 139–157 cal AD 166–195 cal AD 209–258 cal AD 298–320	8,2% 14,1% 33,9% 12,1%	cal AD 130–336	95,4%
UE 11	UBAR-930	1605± 35 BP	cal AD 422	cal AD 415–443 cal AD 449–462 cal AD 483–533	21,9% 8,1% 38,3%	cal AD 386–545	95,4%
UE 14	UBAR-931	1870±130 BP	cal AD 130	cal BC 17– 15 cal AD 0–263 cal AD 276–331	0,4% 58,7% 9,2%	cal BC 195–cal AD 434 cal AD 492–507 cal AD 519–527	94,7% 0,4 0,2%

In the Annex, as additional information, Figure 1 presents a portion of the calibration curve used in the calibration of the radiocarbon dates; this portion of the curve enables to appreciate in the specific chronological region the different incidences and the possible distortion of the radiocarbon chronological scale and also illustrates the calculation of the experimental calibrated dates as the intersection of the experimental radiocarbon date with the calibration curve. Figures 2 show the distribution of probability of the true calibrated dates and enable the appreciation of the intervals with higher probability indicated in columns E and G of table III. Finally, Figures 3 show the accumulated curve of probability that enables to calculate the probability that the true calibrated date is situated in an interval of time as the difference of the ordinates corresponding to the extremes of the interval.

7. Discussion of the Results

The Laboratory wishes to stress that due to its nature, radiocarbon dating dates the formation of the materials and not the events in which these materials were used. The experimental date measured is an approach to a physical date (Mestres, 2000b) that in the case of the dating of charcoal, corresponds to the formation of the vegetable fibres which integrate the vegetable material which later turned into charcoal. In no case, however, does the physical date refer to the archaeological date if this date corresponds to the one when the vegetable elements became charcoal or when the charcoal was deposited in a given archaeological level. For the physical date to correspond to the archaeological date, the association and synchrony requisites must be fulfilled (Mestres, 2000a, 2000b)

Bibliography

MESTRES, J.S. (2000A): "La datació per Radiocarboni. Una visió actual" a *Tribuna d'Arqueologia 1997-1998,* pp. 195-239. Generalitat de Catalunya, Departament de Cultura. Barcelona.

MESTRES, J.S. (2000b): "Utilización inductiva y deductiva de las fechas radiocarbónicas. Ejemplo de aplicación a la prehistoria de la isla de Menorca (Baleares)" a *Contributos das Ciências e das Tecnologias para a Arqueologia da Península Ibérica.* Actas do 3º Congresso de Arqueologia Peninsular, Vol. IX, pp. 117-139. ADECAP, Porto (Portugal).

MESTRES, J.S.; J.F. GARCÍA AND G. RAURET, 1991: "The Radiocarbon Laboratory at the University of Barcelona". *Radiocarbon* **31**(1), p. 23-34.

REIMER, P.J, G.L. BAILLIE, E. BARD, A. BAYLISS, J.W. BECK, C.J.H. BERTRAND, P.G. BLACKWELL, C.E. BUCK, G.S. BURR, K.B. CUTLER, P.E. DAMON, R.L. EDWARDS, R.G. FAIRBANKS, M. FRIEDERICH, T.P. GUILDERSON, A.G. HOGG, K.A. HUGUEN, B. KROMER, G. MCCORMAC, S. MANNIGN, C.B. RAMSEY, R.W. REIMER, S. REMELE, J.R. SOUTHON, M. STUIVER, S. TALAMO, F.W. TAYLOR, J. VAN DER PLICHT AND C.E. WEYHENMEYER. 2004: "IntCal04 Terrestrial Radiocarbon Age Calibration 0–26 cal kyr BP". *Radiocarbon* **46**(3), pp. 1029-1058.

STUIVER, M. AND H. POLACH, 1977: "Discussion: Reporting of 14C Data". *Radiocarbon* **19**(3), p. 358

ANNEX

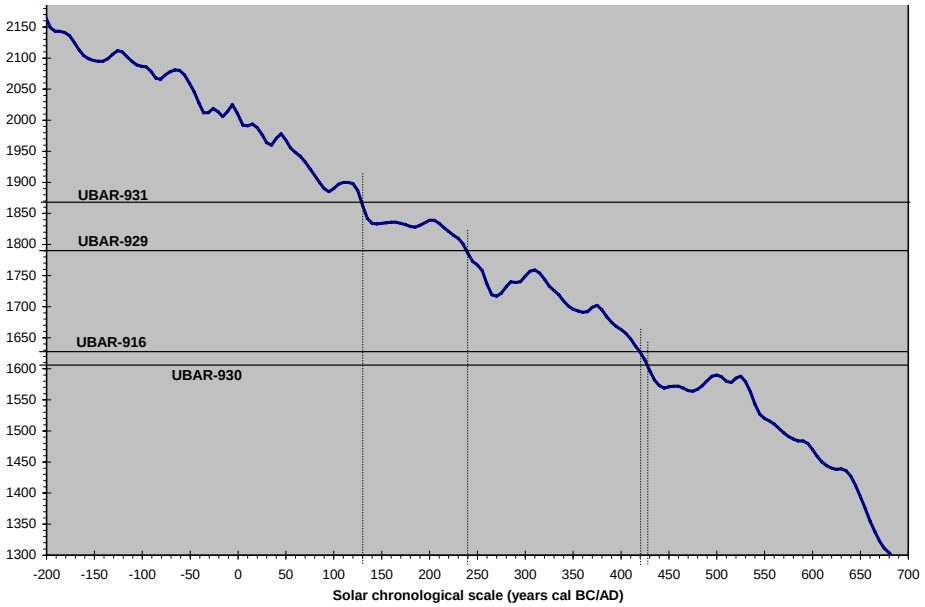

Figure 1

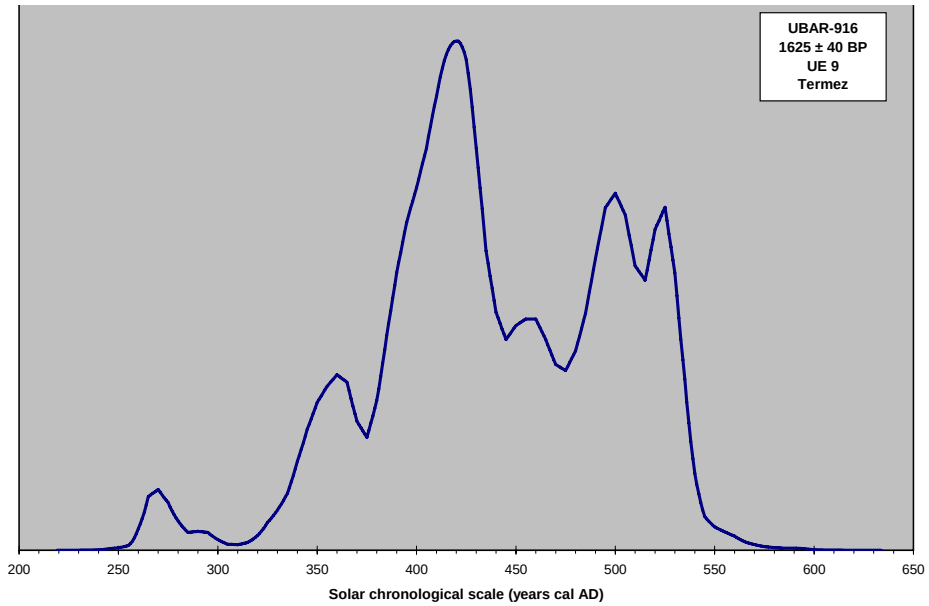

Figure 2A

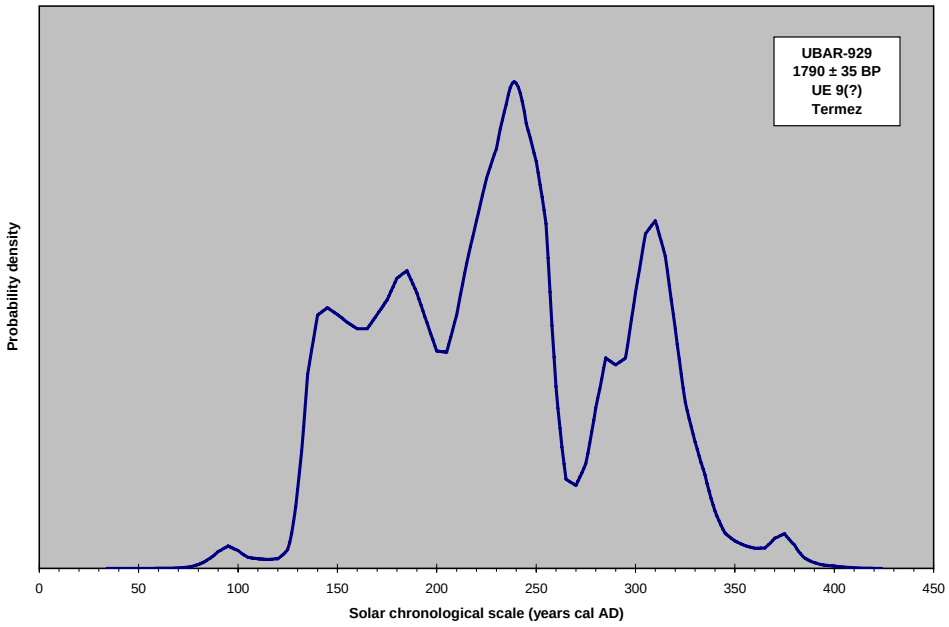

Figure 2B

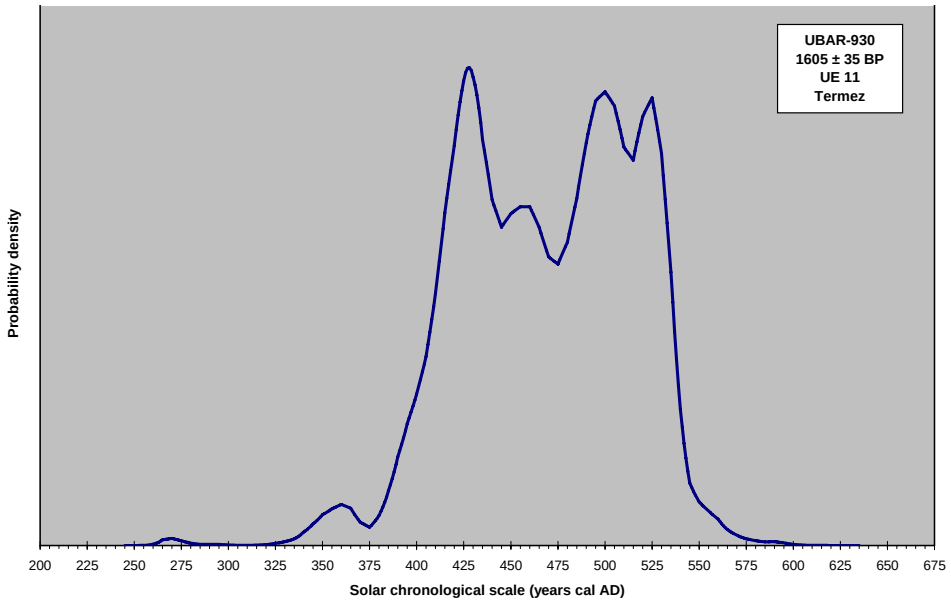

Figure 2C

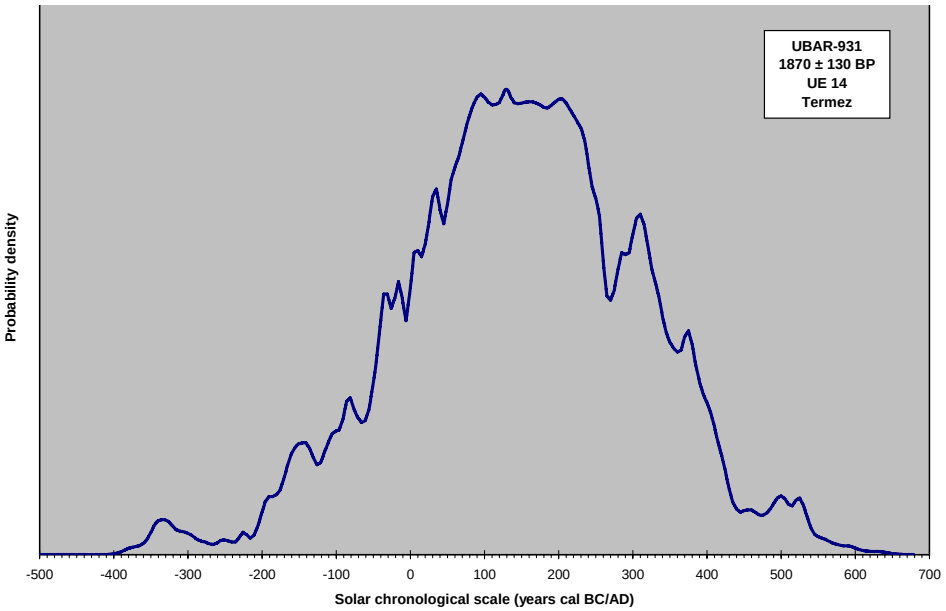

Figure 2D

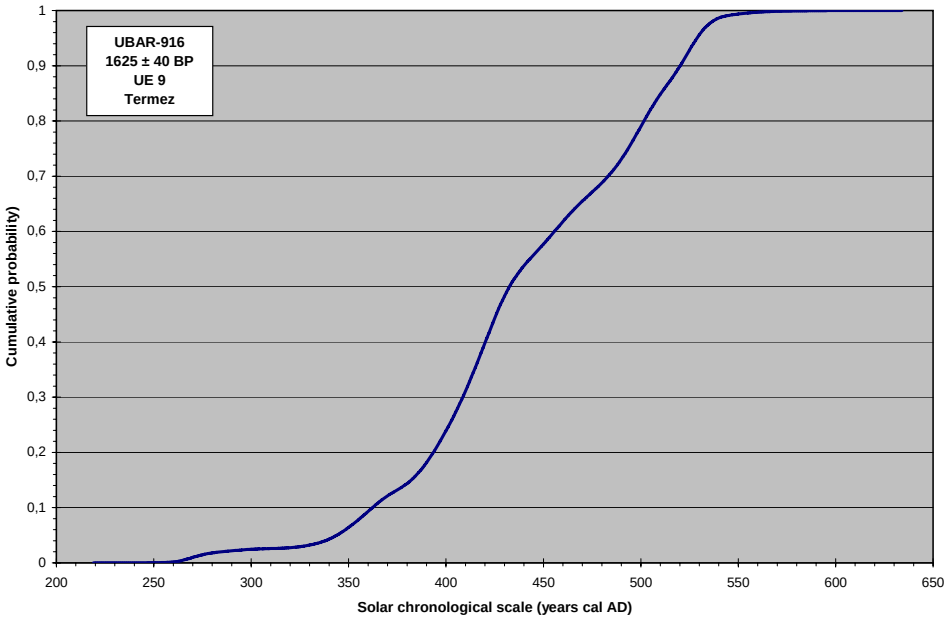

Figure 3A

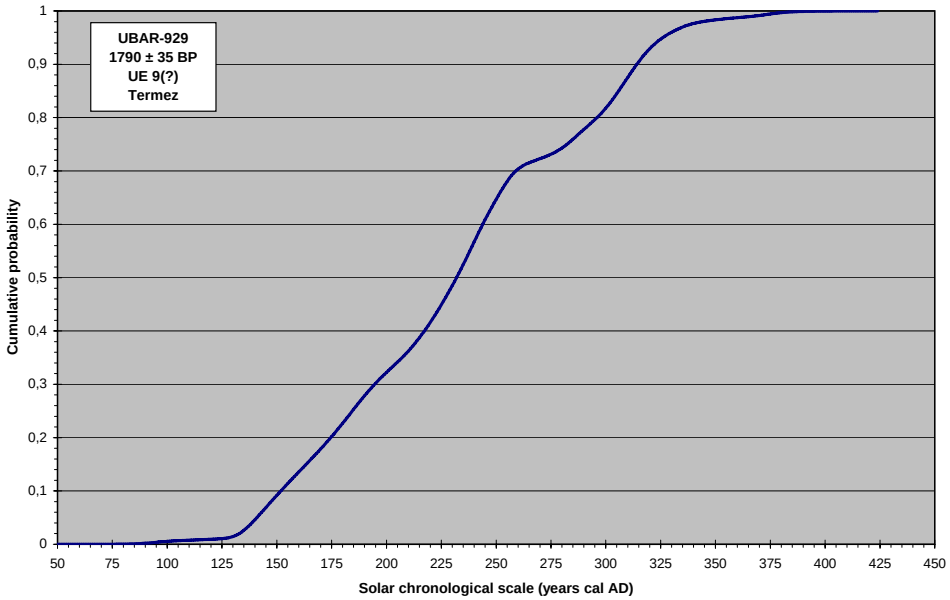

Figure 3B

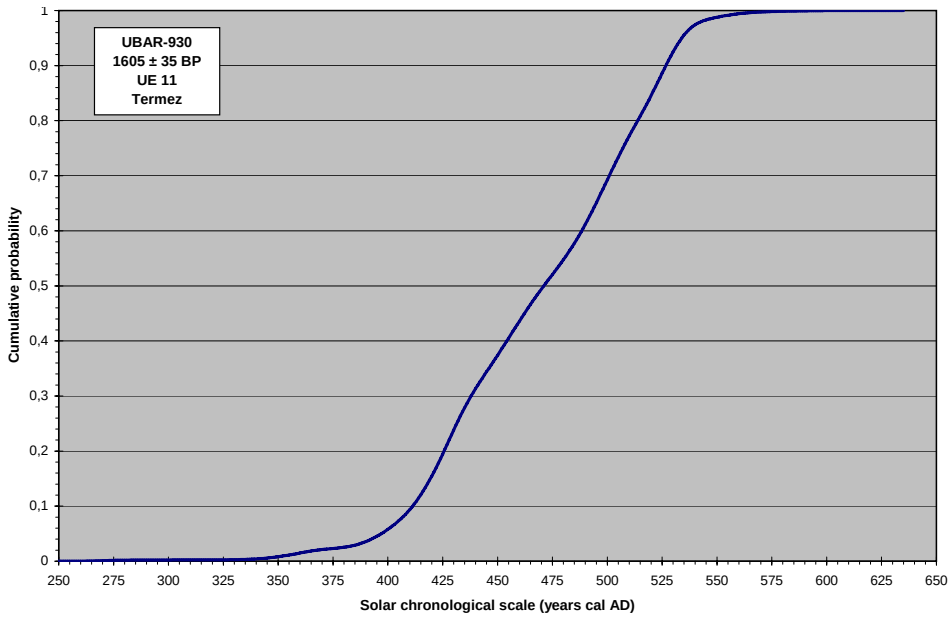

Figure 3C

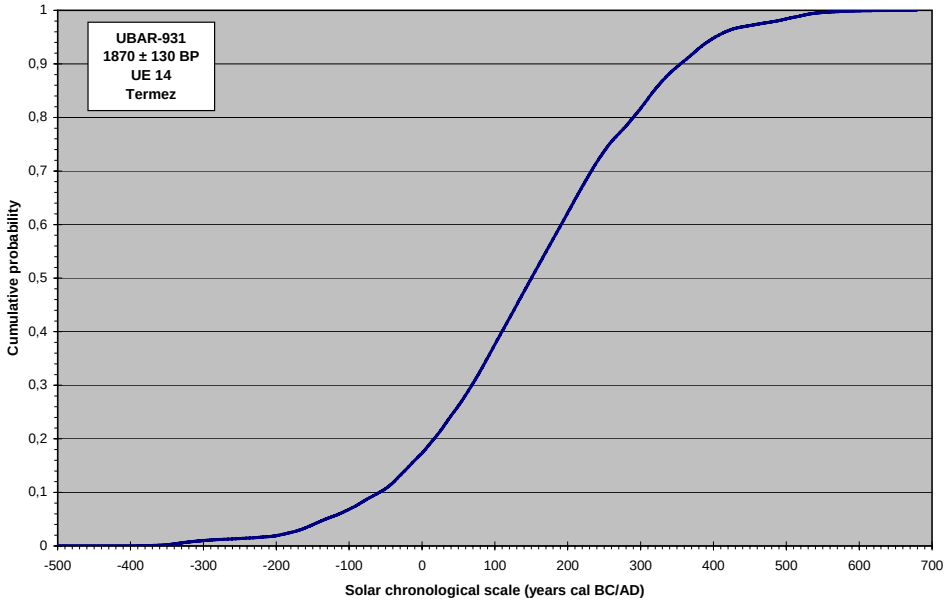

Figure 3D

Final Remarcs

J.M. Gurt, E. Ariño

It is very difficult to evaluate the importance of the ceramic workshop as the geophysical prospections have been done upon a surface of 80 x 30 mts (2400 m2) and at this extension only the existence of one kiln could be confirmed already excavated by the Uzbek-Japanese archeological mission.

Meaning of the stratigraphy inside the laboratory of the kiln and the firing room; there are two different chronological probably successive phases of deposition:

UE 9

Definition	Level of domestic trash
Interpretation	Domestic trash dumped from the kilns' entrance. Contains loess brought by the wind and dumped adobe bricks of the kilns' walls integrated in the layer by the natural progressive and slow destruction process of the kiln.
Observations	Layer composed by loess, adobe bricks, abundant fragmented ceramic material, carbon fragments, ash and bones. The bones are also fragmented and burned, which leads to the hypothesis that this is an intentional deposit formed by trash within the kiln. The entrance of the kiln is covered and it is deeply inclined in the central part. This inclination has been forced to form by the trash dumped into it. Inside there is a baseboard of column made by a calcareous stone.

UE 11

Definition	Layer composed by loess, adobe bricks in a position of have been felled down.
Interpretation	Layer of felled/dumped material formed during the abandonment of the kiln. It presents an exogenous material mostly ceramic fragments and loess brought by the wind.
Observations	Layer composed by loess and adobe bricks. Also contains a great quantity of ceramics. The adobe bricks are fractures and they are in a position of have been felled down. They seem to present different firing temperatures from low (brake when they are touched) to extremely high fired.

The presence of a baseboard of column made by a calcareous stone, with exactly the same fractures than the columns of the monastery located in the surroundings, leads to the hypothesis that, it comes from the destruction level of this same monastery and it vas deposited there at the moment when the monastery does not function anymore. Its position and location inside the kiln indicates that the kiln wasn't functioning at that time either. The C14 results point out that this exact moment must be around the V century A.D. Consequently, it has to be assumed that the ceramic material coming from stuffed material of the kiln and the entrance was fabricated before that date. Even there are no rejected pottery has been found the homogeneous chemical composition of the pottery analysed from the kiln leads us to the conclusion that it was produced at the same production site an that Kiln Nº 1 (excavated by the Uzbek-Japanese mission) and Nº2 were part of the workshop functioned at that site, although there are no clear evidences for that. This fact is transcendent regarding Kara Tepe's pottery because it permits us to define typologically the forms present at this site at the last phase of the existence of the monastery. Therefore, even that the strtigraphical analysis of the Kiln Nº2 indicates two different moments of its stuffing or filling up the ceramic material recovered from the kiln's laboratory area and the firing chamber's area no indicates any difference in chronology, in contrary it can considered as an evidence of the existence of one single horizon formed by homogeneous material.

Brief notes on the palynological samples from Termez

Yannick Miras, Ivan Ivanovich Mal'tsev[1]

A preliminary paleoenvironmental survey took place between the 4th and the 11th of October 2006 in order to evaluate the potential results and investment needed to carry out a serious paleoenvironmental study of Termez.

The aim was to becoming acquainted with the work undertaken by Soviet and Uzbek specialists and to take samples of soils for palynological analysis from the site of Termez and its surrounding environment.

Alluvial terrace of the Surkhan Darya (Site 1)

Site 1 was sampled on 5/10/2006 and named "Amur I". It is a natural section which corresponds to the limit of the first alluvial terrace of the right bank of the Surkhan Darya, situated just to the north of the earth dam, which marks the origin of the main irrigation canal of the plain of Termez. The local environment is marked by the sandy dunes of the Katta Kum desert which reach right up to the river bank.

Fig. 1: Satellite Image of Site 1 (red dot) ; 37°20'53" /67°23'39" ; altitude: 314 m ; Quickbird image 10100100024BD401 taken on 18/09/2003 (source: Google Earth)

1.- The main text, photos and sections are by Y. Miras. The plants were identified by I. I. Mal'tsev.

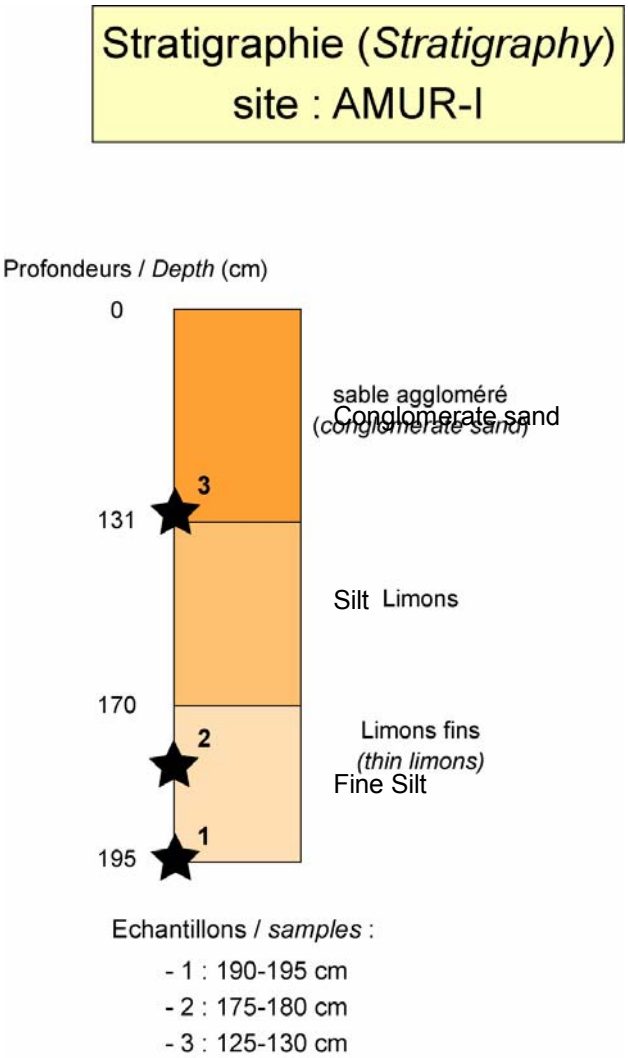

Fig. 2. Stratigraphy and photo of section AMUR-I.

The surrounding vegetation was characterized by the following species[2]:

Scientific name	Quantity (on a 10 point scale)
Calligonum sp	4
Salsola paletzkiana	3
Aellenia subaphylla	4
Girgensohnia oppositiflora	5
Salsola micranthera	3
Agriophyllum latifolium	4
Alhagi canescens	5
Aristida karelinii	3
Tamarix hispida	4
Phragmitis australis	3
Typha latifolia	2
Hordeum murinum	3
Cyperus rotundus	1
Cyperus fuscus	2

2.- The period of the year when the survey took place means that the vegetation was close to its annual minimum and therefore certain species were difficult to identify precisely whilst some annuals may not have been recorded.

Ancient Termez archaeological site

The time spent on the site was minimal (3 hours) and therefore samples were only taken from Tchingiz Tepe.

3 samples were taken from a section dug by the Franco-Uzbek archaeological team (J.-B. Houal) across the ditch situated in front of the eastern fortification wall of Tchingiz Tepe. The site was named “Fossé Kushan I”, the stratigraphical section is continues and composed of loamy sands. The samples were taken at the following depths:

16-26 cm,
170-174 cm,
324-334 cm.

3 samples were taken from a section dug by the Franco-Uzbek archaeological team (S. Mustafakulov) through the corridor of the northern fortification wall. The site was named “Fortification I”

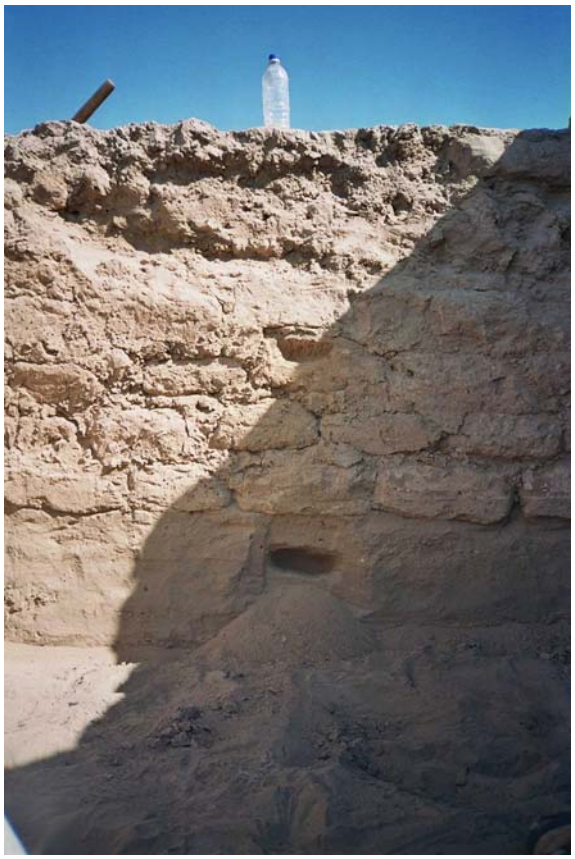

Fig. 3: Photo of the palynological sampling done at the site called: “la nécropole”.

1 sample was taken from a section dug by the Franco-Uzbek archaeological team (Pierre Leriche) in the depression situated to the north of Building B and separating Mala Tchingiz Tepe from Tchingiz Tepe

The surrounding vegetation was characterized by the following species (next page)

Scientific name	Quantity (on a 10 point scale)
Aellenia subaphylla	3
Hammada leptoclada	5
Alhagi canescens	1
Vexibia pachycarpa	2
Koelpinia linearis	3
Cousinia orthacantha	4
Hordeum murinum	5
Vulpia myosuros	3
Bromus oxyodon	2
Bromus tectorum	1
Parentuchelia flaviflora	3
Poa bulbosa	2
Paraver sp.	1
Chrosophora hierusalimica	2
Peganum harmala	1
Haplophylum robustum	2
Helyotropium argusioides	4
Scabiosa olivieri	1
Diarthron vesiculosum	3
Cuminum setifolium	1
Aphanopleura capillifolia	1
Zygophylum atriplicoides	1
Ixiolirion tataricum	1
Allium borszczcowii	1
Ephedra distachia	3
Tribulus terrestris	1
Artemisia diffusa	1
Convolvulus hamadae	1
Ammothamnus lehmannii	1
Cymbolaena griffithiana	1
Lagonichium farctum	2
Leptaleum filifoli um	1

Surveying and sampling in the Bajsuntau Mountains

Finally, in order to evaluate the potential of a proper paleoenvironmental survey, further samples were taken from a peat bog and lacustrine deposits in the Bajsuntau mountain range, situated to the north of Termez at a distance of about 130 kilometers due north.

Ancient Termez on the QuickBird satellite images

S. Stride

A large updata of the satellite imagery in Google Earth and Google Maps was made available on the Third of October 2006[1]. The update included the area around Ancient Termez which passed from low resolution (15 meters) to high resolution (60 cm), enabling the site to be analysed in great detail and a number of features of potential archaeological significance to be identified[2].

This article will concentrate on areas in the vicinity of Ancient Termez, which have not yet been studied, rather than on the site itself. The quality of the satellite images is sufficient for them to be useful to analyse the rest of the site of Ancient Termez, including previously excavated areas such as Fayaz Tepe (see fig. 1).

However, a meaningful analysis based on these satellite images requires them to be integrated with the work of the different archaeological expeditions having worked on the site and in particular with the detailed topographical plan of the site of the MAFOuz de Bactriane. This can be done by draping the satellite images over a 3D topographical model of the site and will be the object of a separate article.

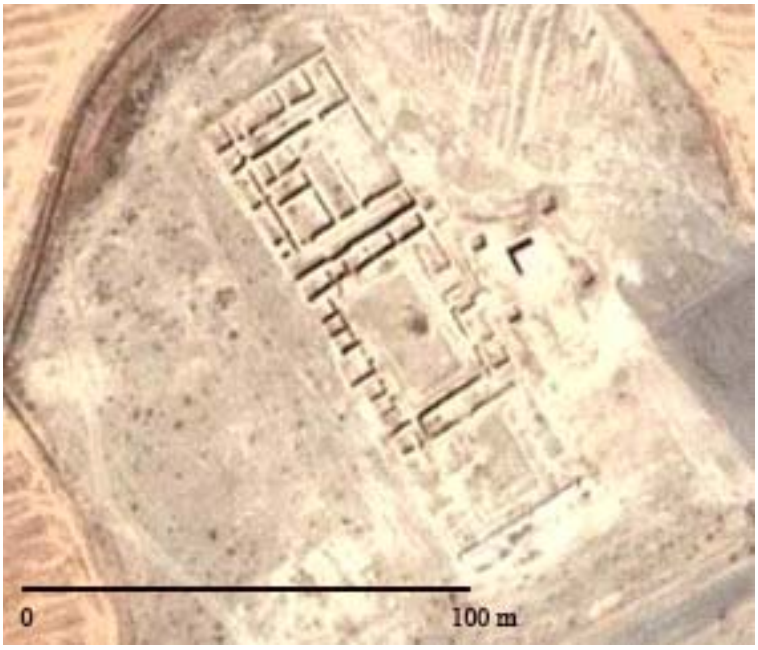

Fig. 1: The site of Fayaz Tepe as seen in Google Earth

Technical characteristics of the satellite images

The images concerning Termez were taken by the Quick Bird satellite and are commercialised by Digital Globe. Their resolution is of 60 cm at nadir in panchromatic[3].

The details of all images concerning Termez can be consulted on Google Earth by activating the "Digital Globe Coverage" layer and clicking for further information on the blue "i" which enables the user to visualise the original satellite image along with the metadata that concerns it.

1.- http://bbs.keyhole.com/ubb/showflat.php/Cat/0/Number/623211

2.- It should be noted that the features recorded on the satellite images have not been verified on the ground.

3.- Detailed characteristics of the QuickBird satellite imagery can be consulted at: http://www.digitalglobe.com/about/quickbird.html

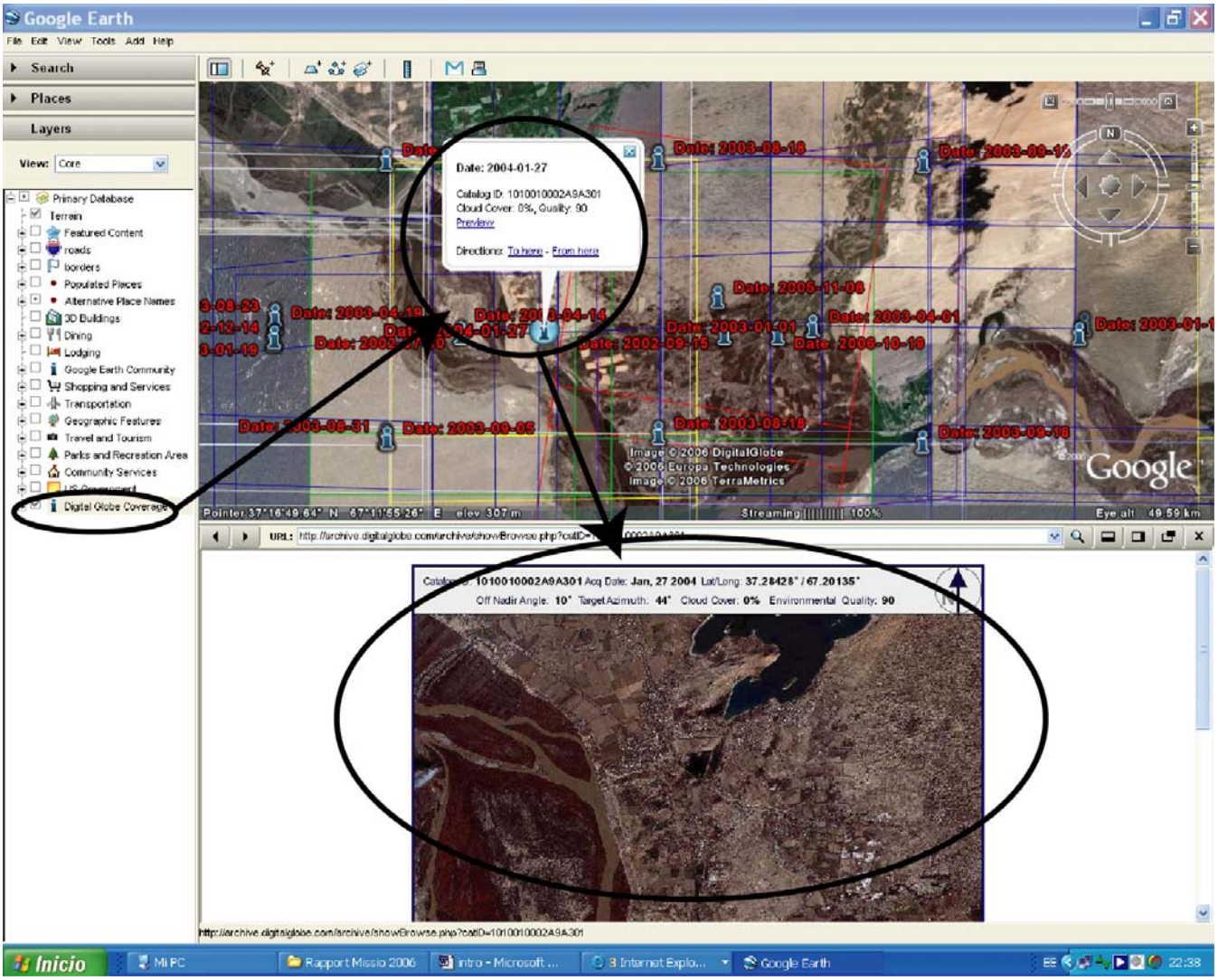

Fig. 2: Screenshot of Google Earth, indicating how to determine the date and characteristics of a giving satellite image

At the time of writing the QuickBird images of Ancient Termez were as follows: 1010010000C2C501 (10/07/2002) ; 1010010002347102 (18/08/2003) ; 10100100023DFE02 (31/08/2003) ; 1010010002427801 (05/09/2003) ; 1010010002A9A301 (27/01/2004).

For the moment it is not possible to select the individual satellite image which one wishes to consult within Google Earth ; however it was possible to determine which of these QuickBird images was included within Google Earth at High Resolution. This was number 1010010000C2C501, taken on the 10th of July 2002[4].

4.- All the illustrations in this article therefore come from this image, or more precisely from the compressed version of this image made available by Google Earth (the Raw Data is not available in Google Earth - for a discussion of this question in an archaeological context see: Beck 2006).

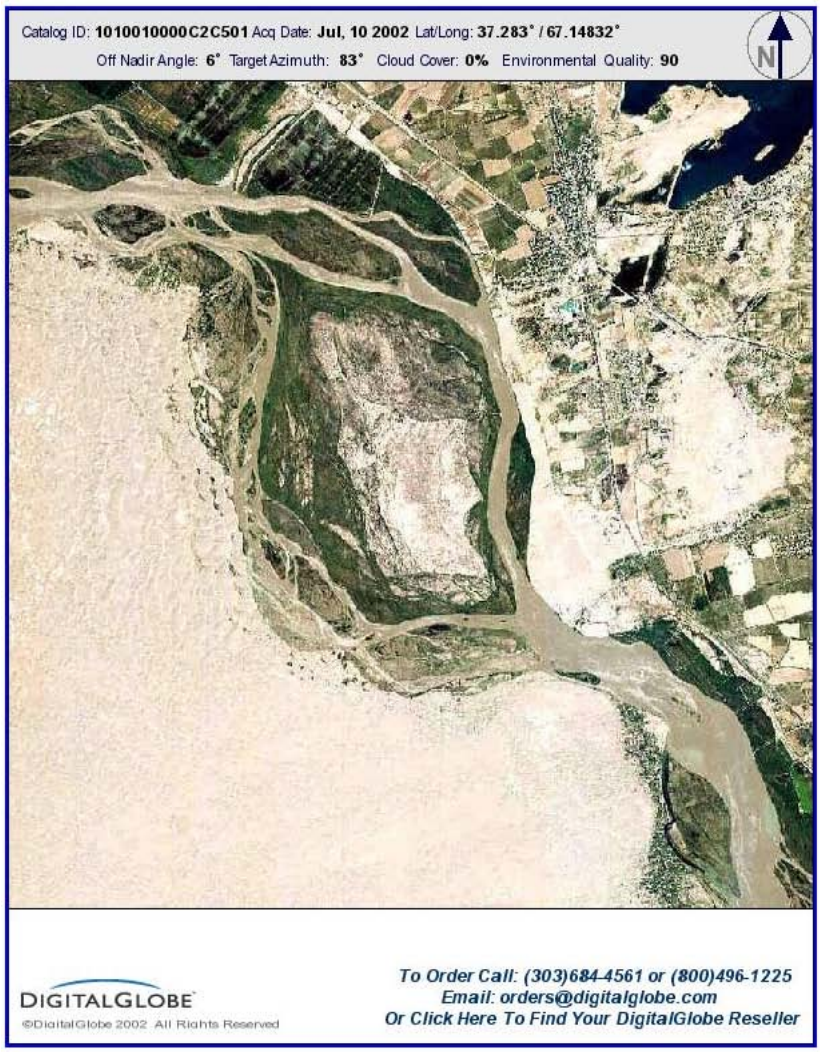

Image Metadata	
ACQUISITION DATE	2002-07-10
CLOUD COVER	0%
CATALOG ID	1010010000C2C501
PAN RESOLUTION	0.62 meters
MULTI RESOLUTION	2.47 meters
ENVIRONMENTAL QUALITY	90 - Excellent
OFF-NADIR	6 degrees
STEREO PAIR ID	NONE

Image Location		
Vertex	Latitude	Longitude
southwest	37.2014	67.0522
northwest	37.3646	67.0522
northeast	37.3646	67.2444
southeast	37.2014	67.2444
center	37.283	67.1483

Close

Fig. 3: The satellite image 1010010000C2C501 from which all other images in this article are taken.

Possible Archaeological Sites on the Afghan side of the Amu Darya

The location of the city of Termez has often been closely linked with the existence of a major crossing point over the Amu Darya river on the main highway linking Samarkand with Balkh / Mazar-e Sharif and Kabul . This crossing point would have been facilitated by the existence of the vast, 5000 hectare, island of Aral Pajgambar, immediately to the West of the ruins of Ancient Termez.

If there was indeed a crossing point over the Amu Darya at Termez, it would make sense for there to be an, or various, archaeological site on the Afghan side of the river. Obviously without a detailed survey nothing definite can be said, however, the QuickBird satellite images do enable us to note a number of interesting features.

Tchingiz Tepe, Kara Tepe and the citadel of Termez are built on natural outcrops of sandstone, which mark the southernmost point of the fault, which separates the Sherabad Darya and the Surkhan Darya basins and is marked further north by the Haudag mountains. The Amu Darya river juts into the citadel of Termez and, for a few hundred meters the river's floodplain disappears on either side. The fact that, unlike further upstream or downstream, the dunes actually reach the river opposite the citadel, on the Afghan side, may well indicate the presence of a sandstone outcrop on this side too.

This feature seems unique, between the Babatag mountains to the East and the Kugitangtau mountains, with Kelif, to the East and reinforces the strategic importance of Termez.

On the Afghan side of the border a number of features could correspond to archaeological sites.

Fig. 4: The Amu Darya river, with the citadel of Termez and possible sites on the opposite side

The clearest candidate is Site 1, situated at 37° 15'15'' / 67° 11'11''. It appears to be a circular site, 85 meters in diameter and straight, orthogonal features, presumably corresponding to walls, can be clearly seen on the main mound. Finally, a large lineal elevation of some 600 meters in total, may correspond to the fortification wall of a hypothetical lower town, the northern part of which may have been washed away by the river.

The second candidate is situated to the West of the first one, at 37° 15'12'' / 67° 10'32''. It appears

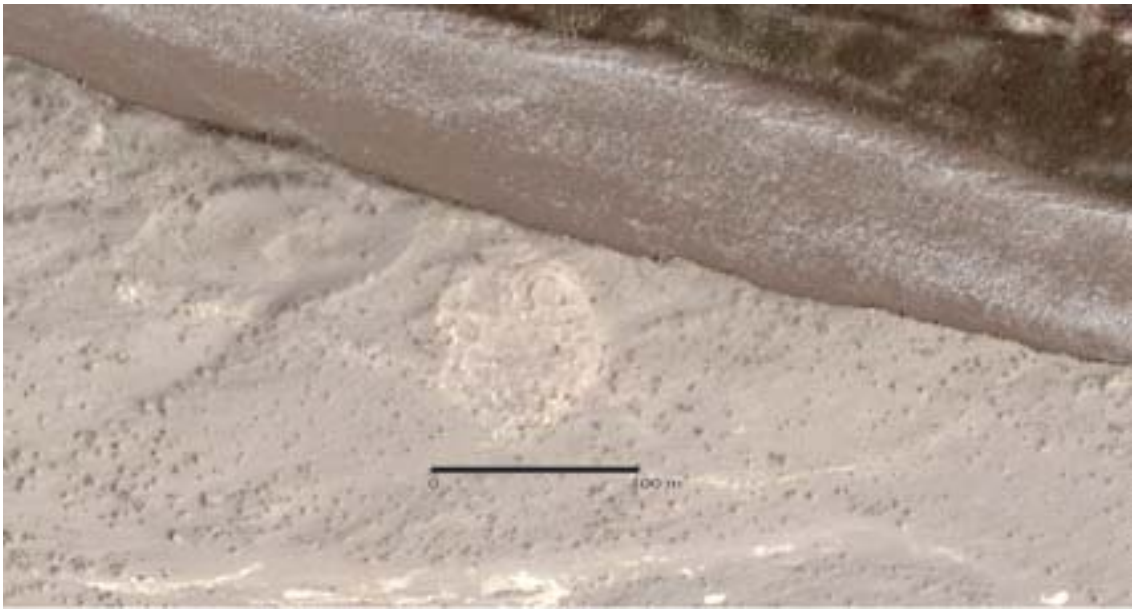

Fig. 5: Site number 1 on the Afghan side

to be a rectangular site (90x35 m), with traces of what may be walls in a number of places, notably along the South-East side.

The third possible site (37° 15'12'' / 67° 11'38'') is situated 700 meters SEE of the first site and 120

Fig. 6: Site number 2 on the Afghan side

meters West of the fourth possible site (37° 15'03'' / 67° 11'45''). Both sites clearly correspond to man-made features (number 3: 45x30 m, number 4: 40x35 m) and are may have been domestic compounds with an exterior wall, living quarters and barns. it is impossible to date them from the satellite image alone and they could prove to be recent[5].

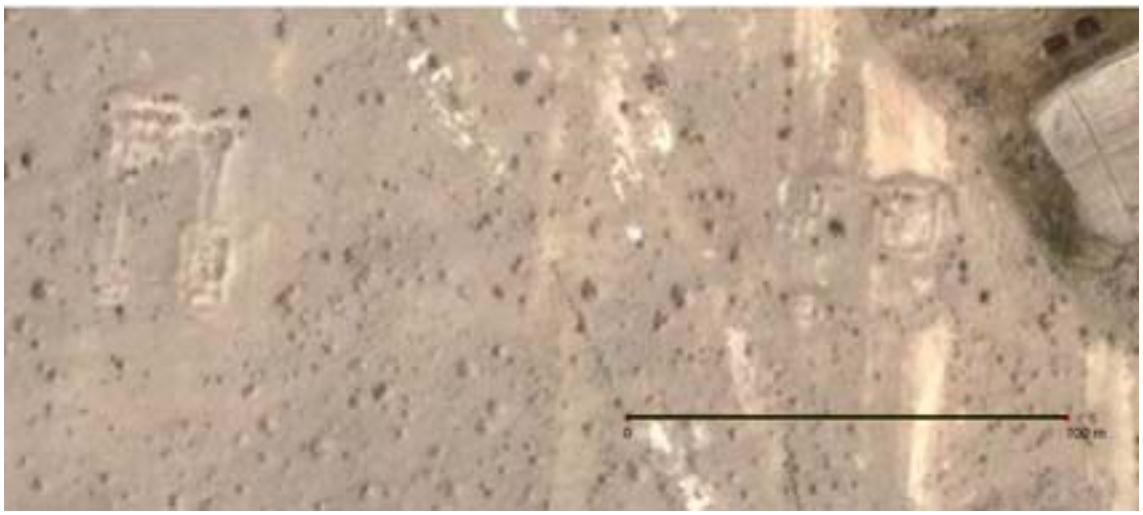

Fig. 7: Site number 3 and 4 on the Afghan side

5.- Both sites have a number of features in common with existing buildings in the irrigated plain situated just to the east.

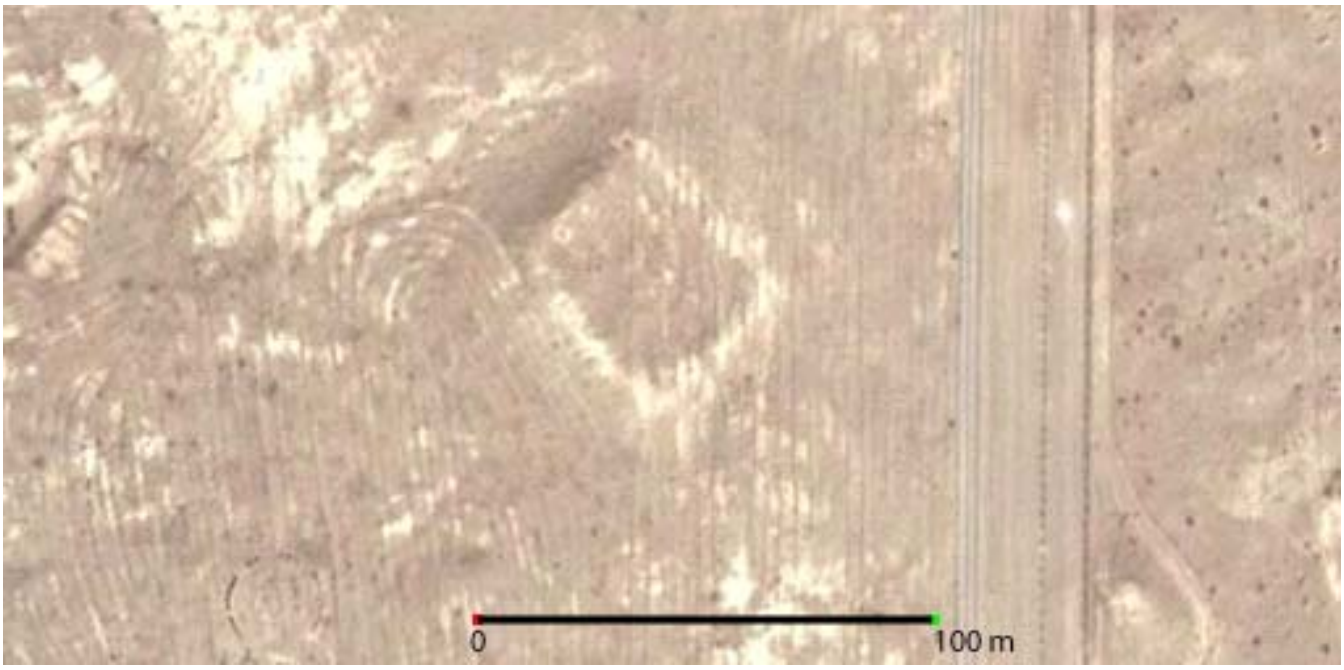

Fig. 8: Large structure to the north of Tchingiz Tepe, in the military zone

North of Tchingiz Tepe

The area North of Tchingiz Tepe and on the river side of the border has been very little explored. Mentions are made of a number of naus. The satellite image clearly shows a large (47x40 m), rectangular, man-made structure at 37° 16'31'' / 67° 10'47'', which has not, to our knowledge, been previously reported.

The oasis wall of Termez

One of the major topographical features of Ancient Termez is a long elevation running East-West and passing just to the North of Kara Tepe. It is already indicated on the plan drawn by the TAKÈ expedition in the late 1930's and can clearly be seen on the satellite images from 37° 16'44'' / 67° 10'36'' in the West up to 37° 16'55'' / 67° 11'54'' in the East.

Fig. 9: Main oasis walll to the north of Kara Tepe

6.- See Kastal'skij 30a (p.19, canal) ; Masson, M. 41 (pp.89-91, 93) ; Shishkin 41 (pp.127, 150) ; Nikolaev 72 ; Al'baum 74 (p.57) ; Al'baum 76 (p.45) ; Al'baum 85' ; Al'baum 90a' ; *Mkrtychov 94 (p.119) ; Staviskij 98 (pp.44-45)

Over the years various interpretations of the topographical feature have been suggested, including that of it having been a canal, alimented by water wheels from the Amu Darya and a outer fortification wall[6] Recent excavations by Sh. Pidaev seem to prove fairly conclusively that the elevation should be interpreted as a wall and dated to the Kushan period (pers. com.).

Fig. 10: Possible continuation of the oasis wall further to the east of Ancient Termez

What is interesting on the QuickBird image is that there appears to be a structure further to the East, which is almost perfectly aligned with this topographical feature and oriented in the same east-west direction (it can be easily traced from 37° 17'11'' / 67° 13'22'' in the West up to 37° 17'30'' / 67° 14'08'' in the East).

The remains are not as clear and will need to be investigated in the field, however they would seem to form part of the same long east-west feature.

If, as all available evidence indicates, it is indeed a wall, then it is unlikely to have been part of the fortifications of the city of Termez itself (the eastern limit of the visible section is situated at 5 km north-east-east of the citadel and there is no reason to think that it stopped at this point). The comparisons which spring to mind are those with outer oasis walls such as the Antiochus and Gilyakin-Chilburj walls around Ancient Merv, the Kampyryak around Bukhara, the Kampyr Diwal in the vicinity of Samarkand and those of many other sites in Central Asia[7].

We therefore think that this structure materialises the outer limit of the oasis of Termez (fig. 10 clearly shows how it marks the limit between the irrigable area to the South and the desert to the North). As such it is likely that it originally reached right up to the Surkhan Darya, not far from the point where the Termez Canal has its origin.

7.- See Bader, Callieri, Khodzhaniyazov 1998 on the walls of Merv, with discussion and bibliography of the other sites. Of course the oasis wall of Termez would enclose a smaller area than most of the other ones but this is to be expected in light of the size of the oasis of Termez.

References

AL'BAUM, L. I., 1974, "Raskopki buddijskogo kompleksa Fajaz-tepe (po materialam 1968-1972 gg.)", in : *Drevnjaja Baktrija*, pp. 53-58.

AL'BAUM, L. I., 1976,"Issledovanie Fajaztepe v 1973 g.", in : *Baktrijskie drevnosti*, pp. 43-45.

AL'BAUM, L. I., 1985, "K voprosu ob istoricheskoj topografii gorodish Starogo Termeza", in : *Tvorcheskoe nasledie narodov Srednej Azii v pamjatnikakh iskusstva, arkhitektury i arkheologii*, pp. 11-12.

AL'BAUM, L. I., 1990, "Raskopki na gorodishche Staryj Termez (1976-1989)", in : *Arkheologija Srednej Azii*, pp. 23-25.

BADER, A., CALLIERI, P., KHODZHANIYAZOV, Y., 1998, "Survey of the "Antiochus Wall" Preliminary Report on the 1993-1994 campaigns" in: *The Archaeological Map of the Murghab Delta*, A. Gubaev, G. Koshelenko, M. Tos i ed., Roma, IsIAO, pp. 159-186.

BECK, A., 2006, "Google Earth and World Wind: remote sensing for the masses?", *Antiquity* 80, no 308. Online at: http://www.antiquity.ac.uk/ProjGall/beck/index.html

KASTAL'SKIJ, B. N., 1930, "Istoriko-geograficheskij obzor Surkhandar'inskoj i Sherabadskoj dolin (Obzor ostatkov pamjatnikov material'noj kul'tury v Surkhanskoj i Shirabadskoj dolinakh)", *VIR*, 1930/3, pp. 3-19.

MASSON, M. E., "Gorodishcha Starogo Termeza i ikh izuchenie", in : *TAKÈ I*, 1941, pp. 5-122.

MKRTYCHOV, T. K., 1994, "Buddhist ritual practice of Kara Tepe (based on materials of complex E)", *SRAA* 3 (1993/1994), pp. 97-112.

NIKOLAEV, V. P., 1972,"Issledovanie vneshnego vala gorodishcha Starogo Termeza (1969 g.)", in : *Kara-tepe III*, pp. 62-66, ill. 17.

SHISHKIN, V. A., "K istoricheskoj topografii Starogo Termeza", in : TAKÈ *I*, 1941, pp. 123-153.

STAVISKIJ, B. JA., 1998, *Sud'by buddizma v Srednej Azii (po dannym arkheologii)*, Moskva, RAN.

Main results, Projects and Requirements for 2007

J.-M. Gurt, Sh. Pidaev, S. Stride

The first season's work has proven extremely promising with a number of important field results and the promise of results from laboratory analysis over the coming months.

We are now able to define in much greater detail the future developments of our activities and also our financial requirements.

Analysis of the material (winter 2006-2007)

During the 2006 season we collected a number of samples in the field, including charcoal, ash, soil and sherds from the excavation of the kiln at Termez ; soil samples and animal excrements from Termez, the terraces of the Amu Darya, the Sherabad Darya valley and the Bajsuntau mountains.

These samples have been exported from Uzbekistan to Barcelona in order to be analysed during the coming winter as follows:

Archaeometrical analysis

A total of 50 sherds from the excavation of the kiln will be analysed by E. Tsantini and V. Martinez. The analysis will be done by Scanning Electron Microscope, X Ray Diffraction and X-Ray Fluorescence. To our knowledge, it will be the first systematic analysis of this type undertaken on Kushan period sherds from any site in Central Asia, Afghanistan, Pakistan of Northern India. It will enable us to obtain a reference collection, which will then be compare with material from the site of Termez itself and from neighbouring sites.

Radiocarbon dating

Various samples were taken during the excavation of the kiln at the site of Termez in order to obtain radiocarbon dates of the period of abandon – and maybe – also of use of the kiln. These will provide important benchmarks for the excavation but also for the absolute chronology of Kushan pottery, a question, which remains much debated.

Palynological samples

The palynological samples will be analysed by Y. Miras during the year 2007 so as to evaluate the degree of preservation of pollen in the different environments where samples were taken (and thus the areas where a detailed palynological study can be undertaken and the quality of the results, which we can hope to obtain from such a study). It will also make it possible to propose a preliminary reconstitution of the environment in the vicinity of Ancient Termez and to collate the data obtained with the vegetation chart established by A. Maltseev.

Preliminary missions

Invitation of Uzbek Scholars

In spring 2007, two Uzbek scholars will be invited to Barcelona for a period of two weeks. During this time, they will follow a formation course on archaeometrical techniques and will impart a conference on their work in Central Asia.

Spring season 2007

In May 2007 the results of the work of the IPAEB will be presented at an International Congress organised by the Academy of Sciences of Uzbekistan in Samarkand.

During our stay we will also work at the Institute of Archaeology in order to evaluate the possibility of creating a laboratory of archaeometry at Samarkand and will attempt to acquire detailed topographical maps of Termez and the Bajsuntau mountains.

Field season 2007

The main field season will take place in September 2007 and will include the following parts:

Geophysical Survey

The results of the geophysical survey have proven satisfactory (see above) and will therefore be extended. In 2007, we plan to survey the rest of Tchingiz Tepe using the georadar, and also to undertake a survey of the area surrounding the stupa of Zurmala where most specialists believe that a major Buddhist monastery could have been localised.

Excavation of Tchingiz Tepe

The preliminary results of the geophysical survey of Tchingiz Tepe make it possible to plan an excavation of the site in collaboration with the Franco-Uzbek Mission currently working there. The two main aims will be the verification of the hypothesis of a return of the fortification wall along the ravine situated to the South-East of the site and a test trench on a domestic area so as both to verify the geophysical data and excavate a precise statigraphical sequence from which we can obtain material for archaeometrical and other types of analysis (including radiocarbon datation).

Excavation of the ceramic production area

The excavation of the ceramic production area, situated next to Kara Tepe, will be continued with the following aims:

- To date the period of construction of the kilns by excavating the previous levels of occupation
- To analyse in more detail the extension of the ceramic production area and to evaluate the number of kilns.
- To excavate at least one more kiln so as to evaluate the degree of standardisation of these
- To localise and excavate an area where discarded production from the kilns was dumped so as to obtain material, which we can definitively attribute to these kilns.
- To excavate the structures that were brought to light by the geophysical survey.

Survey of the sites in the Termez area

The analysis of the QuickBird satellite images and the catalogue of sites created for the Termez area that will be published by UNESCO, make it possible to plan a detailed survey of the area of Termez. This will include the following elements:

- Verification of the localisation of all the sites recorded in the gazetteer.
- Integration of the GIS of the Termez area with Google Earth thanks to a plugin.
- Installation of a version of this GIS at the Termez Museum, which will be used by the Uzbek
- Commission for the Preservation of the Cultural Heritage.
- Field study of the elements recorded on the QuickBird satellite images

Investigation of the Afghan side of the Amu Darya

If it proves possible, we aim to undertake a survey of the Afghan side of the Amu Darya river, opposite Termez so as to investigate the sites seen in the satellite images and evaluate their relationship with the city of Ancient Termez.

Congresses and diffusion of our activities

An important part of the project concerns the diffusion and publication of our activities. The following are the main points of these activities so far:

Scientific Publications

Although our research has only just started, we have a number of publications planned and one already in press.

In press:
Sh. Pidaev, S. Stride *Master Plan for the Conservation of the Cultural Properties of Termez*, Tashkent, UNESCO, 2007, 150 p., 80 ill.

In preparation:
- J.-M. Gurt, Sh. Pidaev, S. Stride et al. "The first season of the catalano-uzbek archaeological excavation", in *Istorija Materialnaja Kul'tura Uzbekistana*. (This article will be published in Russian in the main archaeological journal of the Uzbek Academy of Sciences)
- J.-M. Gurt, Sh. Pidaev, S. Stride et al. *First Season of the Catalano-Uzbek Archaeological Mission*. (This monograph will be based on the scientific part of the report and will be published both online and in paper format in spring 2007)

Congresses

The existence of the Catalano-Uzbek Archaeological Mission has enabled us to organise a major meeting in Barcelona, which took place on the 14th and 15th of December 2006.

This meeting, organised by the University of Barcelona with the collaboration of the CIDOB and the University of Milan Bicocca was be chaired by S. Stride, B. Rondelli and G. Vizzari and entitled: ***First International Workshop for the Creation of an Archaeological Information System of Central Asia***.

It was directed at young scholars and PhD students and over 30 people took part from the leading universities and research centres of Austria, the Czech Republic, France, Germany, Italy, Japan, Spain, the United Kingdom and the United States.

The results will be published both online and in paper format and the workshop will formalise the creation of a network of institutions and scholars involved in Central Asian Studies.

Courses

The work of our team has also been one of the reasons for the creation of a general introductory course on the History of Eurasia and the Silk Roads of 6 credits at the Department of Prehistory, Ancient History and Archaeology. This course will hopefully be fully integrated into the curriculum of the Department from the year 2007-2008.

Conferences

The results of our work have been presented informally at a the French Institute of Anatolian Studies in Istanbul, the French Institute of Central Asian Studies in Tashkent, a seminar in the University of Milan Bicocca, the Altaveu cycle of the Amics de l'UNESCO and a conference on the Serial Nomination of the Silk Roads to the World Heritage List organised by the UNESCO at Samarkand.

Financial Requirements

We are convinced that our first season of work has proven beyond doubt the interest and potential of the Catalano-Uzbek Mission. However, it is clear that working in an area such as Central Asia, on a project of this nature is not possible in the Medium or Long Term without a substantial increase in our finances.

In order to function successfully in the field (in particular to increase the number of participants in the expedition – both professional and students), to be able to afford the analysis of material in the laboratory and to transfer state of the art technology to our Central Asian colleagues we need to double the basic finance of our team from 23 000 euros per year to 46 000 euros per year.

We also feel that there it is important to create a strong research group in Barcelona, specialised in Central Asia and on the Silk Road.

The creation of an International Network of scholars, which will be coordinated by a member of our team and the organisation of a meeting of specialists from Europe, Japan and the United States at Barcelona opens a unique window of opportunity. Unlike in other parts of Asia where Spanish research

is just starting and is still far from being on an equal par to the traditions of other European, Asian or North American countries, we can position ourselves in Central Asia as one of the leading International Teams.

In order to succeed, we must create a proper structure, develop classes on Central Asia and the Silk Road, invite professional from abroad, enable students from Spain to travel to Central Asia.

Of course, all of this requires money, but the amount invested seems to us minor when compared to the potential benefits, for the image of Spain and Catalonia, for the international cooperation which our work implies, for our understanding of the long term contacts between civilisations, for developing a new way of looking at our own history and for the technical and methodological innovations, which we are implementing.